

NASA CR- 134627



HIGH-TEMPERATURE, LOW-CYCLE FATIGUE
OF ADVANCED COPPER-BASE ALLOYS
FOR ROCKET NOZZLES; PART I -
NARLOY Z.

by: J.B.Conway, R.H.Stentz and J.T.Berling

MAR-TEST INC.

Cincinnati, Ohio

May, 1974

prepared for

NATIONAL AERONAUTICS AND SPACE ADMINISTRATION

NASA Lewis Research Center
Contract NAS3-17777

G.R.Halford, Project Manager

(NASA-CR-134627) HIGH-TEMPERATURE,
LOW-CYCLE FATIGUE OF ADVANCED COPPER-BASE
ALLOYS FOR ROCKET NOZZLES. PART I:
NARLOY Z (Mar-Test, Inc., Cincinnati,
Ohio.)
CSCL 11D

G3/17
Unclas
40155

N74-26023

1. Report No. NASA CR 134627		2. Government Accession No.		3. Recipient's Catalog No.	
4. Title and Subtitle High-Temperature, Low-Cycle Fatigue of Advanced Copper-Base Alloys for Rocket Nozzles; Part I - Narloy Z				5. Report Date May 1974	
				6. Performing Organization Code	
7. Author(s) J. B. Conway, R. H. Stentz and J. T. Berling				8. Performing Organization Report No. MTI- R003 - 3 - 1	
9. Performing Organization Name and Address Mar-Test Inc. 45 Novner Drive Cincinnati, Ohio 45215				10. Work Unit No.	
				11. Contract or Grant No. NAS3-17777	
12. Sponsoring Agency Name and Address National Aeronautics and Space Administration Lewis Research Center 21000 Brookpark Rd., Cleveland, Ohio 44135				13. Type of Report and Period Covered Contractor Report January through Feb. 1974	
				14. Sponsoring Agency Code	
15. Supplementary Notes Project Manager, Dr. G. Halford, NASA-Lewis Research Center Cleveland, Ohio					
16. Abstract <p>Short-term tensile and low-cycle fatigue data are reported for Narloy Z, a centrifugally cast, copper-base alloy developed by North American Rockwell. Tensile tests were performed at room temperature in air and in argon at 482°, 538° and 593°C using an axial strain rate of $2 \times 10^{-3} \text{ sec}^{-1}$. In addition tensile tests were performed at 538°C in an evaluation of tensile properties at strain rates of 4×10^{-4} and $1 \times 10^{-2} \text{ sec}^{-1}$. Ultimate and yield strength values of about 315 and 200 MN/m² respectively were recorded at room temperature and these decreased to about 120 and 105 respectively as the temperature was increased to 593°C. Reduction in area values were recorded in the range from 40 to 50% with some indication of a minimum ductility point at 538°C.</p> <p>Strain-controlled low-cycle fatigue tests were performed in argon at 538°C to define the cyclic life over the range from 100 to 3000 cycles using a strain rate of $2 \times 10^{-3} \text{ sec}^{-1}$. Other tests were performed at this same temperature to define the effect of strain rate on the fatigue life at strain ranges of 0.9 and 2.6 percent. Definite saturation effects were indicated in both the low and high strain rate regimes.</p> <p>Low-cycle fatigue tests were performed to evaluate temperature and hold-time effects. Little to no temperature effect was observable over the range from 482° to 593°C in the higher strain range regime but a definite temperature effect was noted at a strain range of 0.90%. Hold periods (300 seconds duration) in tension at 538°C were found to have a very detrimental effect on fatigue life whereas hold periods in compression appeared to yield a somewhat greater fatigue life than that observed in continuous cycling tests.</p> <p>Relaxation data obtained during a hold period near half-life are reported for each specimen tested with a hold period. Relaxation in the 300-second hold periods appears to be essentially the same for the tensile and compression hold periods.</p>					
17. Key Words (Suggested by Author(s)) Fatigue, Tensile, Hold-Time, Strain Rate, Temperature, Relaxation, Crack Initiation Copper-base Alloys			18. Distribution Statement unclassified-unlimited		
19. Security Classif. (of this report) unclassified		20. Security Classif. (of this page) unclassified		21. No. of Pages	
				22. Price*	

* For sale by the National Technical Information Service, Springfield, Virginia 22151

TABLE OF CONTENTS

	<u>page</u>
I - SUMMARY	1
II - INTRODUCTION	3
III - MATERIAL AND SPECIMENS	6
IV - TEST EQUIPMENT	8
V - TEST PROCEDURES	13
A) Low-cycle Fatigue	13
B) Short-Term Tensile	16
VI - TEST RESULTS AND DISCUSSION OF RESULTS	17
A) Short-Term Tensile	17
B) Low Cycle Fatigue	17
1) Continuous Cycling Behavior at 538°C and a Strain Rate of $2 \times 10^{-3} \text{ sec}^{-1}$	17
2) Strain Rate Effects at 538°C	22
3) Temperature Effects	31
4) Hold-Time Effects at 538°C	31
5) Relaxation Behavior	37
VII - CONCLUSIONS	44
DISTRIBUTION LIST FOR THIS REPORT	46

1 - SUMMARY

This report describes the test results obtained in the Task 1 portion of this program which involved an evaluation of the short-term tensile and low-cycle fatigue behavior of Marloy Z. This copper-base alloy was developed by North American Rockwell and was furnished as centrifugally-cast, hot rolled, solution-annealed and aged plate material. Hourglass-shaped specimens were employed in tests which were performed in air at room temperature and in high purity argon (oxygen level below 0.01 percent by volume) when elevated temperatures were involved.

Duplicate tensile tests were performed at room temperature, 482° and 538° using a nominal axial strain rate of $2 \times 10^{-3} \text{ sec}^{-1}$. In addition, tests were performed at 538° using axial strain rates of 4×10^{-4} and $1 \times 10^{-2} \text{ sec}^{-1}$. These test results indicated room temperature ultimate and yield strengths at a strain rate of $2 \times 10^{-3} \text{ sec}^{-1}$ of 315 and 200 MN/m² respectively and a gradual decrease in these values to 120 and 105 MN/m² as the temperature increased to 593°. Reduction in area values at this same strain rate remained constant at about 50% over the range from room temperature to 593° except for a minimum ductility point at 538° when the reduction in area value of 42 percent was obtained. Strain rate was observed to have a very significant effect on the ductility at 538° as the reduction in area values increased from about 34 percent at a strain rate of $4 \times 10^{-4} \text{ sec}^{-1}$ to 51 percent at a strain rate of $1 \times 10^{-2} \text{ sec}^{-1}$. In this same strain rate regime very little effect was noted on the yield strength while a 20 percent increase in ultimate strength was indicated as the strain rate increased to $1 \times 10^{-2} \text{ sec}^{-1}$.

A series of low-cycle fatigue tests was performed at 538° using a strain rate of $2 \times 10^{-3} \text{ sec}^{-1}$ to define the fatigue life over the range of 100 to 3000 cycles. This required a strain range regime from about 3.5 percent to 0.7 percent. Additional tests were then performed at selected strain ranges of 0.90 and 2.6% to evaluate the fatigue life at strain rates from 4×10^{-4} to $5.2 \times 10^{-2} \text{ sec}^{-1}$. These data identified a definite strain rate effect on fatigue life and one that exhibited a trend toward saturation at both the low and high values of strain rate.

A limited study of the effect of temperature on the fatigue life of the R-24 alloy was performed at strain ranges of 0.90 and 2.6 percent using a strain rate of $2 \times 10^{-3} \text{ sec}^{-1}$. These tests indicated little to no effect of temperature over the range from 482° to 593° when the strain range was 2.6 percent but a very definite temperature effect over this same temperature range when the strain range was 0.90 percent.

A hold period duration of 300 seconds was employed in an evaluation of hold-time effects at 538° for strain ranges of 0.90 and 2.6 percent. Hold periods in tension were found to be very

detrimental and led to noticeable decreases in fatigue life particularly at the lower strain range. Hold periods in compression were not found to be detrimental but rather seemed to increase the fatigue life to values slightly greater than those observed in the continuously cycling tests.

Relaxation data are reported for each test. A cycle near half-life was selected and a relaxation curve for this cycle is presented to provide a comparison of the observed relaxation behavior.

II - INTRODUCTION

Regeneratively-cooled, reusable-rocket nozzle liners such as found in the engines of the Space Shuttle, Orbit-to-Orbit Shuttle, Space Tug, etc., undergo a severe thermal strain cycle during each firing. To withstand the severe cycles, the liner material must have a proper combination of high thermal conductivity and high low-cycle fatigue resistance. Copper-base alloys possess these desirable qualities and were thusly chosen for this program. A broad-based NASA-Lewis/MAR-TEST program has been instituted to evaluate several candidate alloys by generating the material property data that are required for the design and life prediction of rocket nozzle liners. This report deals almost exclusively with the tensile and high-temperature, low-cycle fatigue behavior of one copper-base alloy, NARloy Z. This alloy was developed by North American Rockwell for use as a rocket nozzle liner material and was evaluated in this program in the hot-rolled, solution annealed and aged condition. Specimen blank material was supplied in the form of a 25 cm x 23 cm x 4 cm plate and for this program this material was given the code designation R-24.

The material property evaluations specified for this Task 1 effort were as follows:

- 1) duplicate tensile tests at room temperature, 482° , 538° and 593° using a nominal axial strain rate of $2 \times 10^{-3} \text{ sec}^{-1}$;
 - 2) duplicate tensile tests at 538°C using nominal axial strain rates of 4×10^{-4} and $1 \times 10^{-2} \text{ sec}^{-1}$;
 - 3) six completely reversed, axial strain controlled low-cycle fatigue tests at 538°C using an axial strain rate of $2 \times 10^{-3} \text{ sec}^{-1}$ to define the fatigue life over the range from 100 to 3000 cycles;
 - 4) duplicate low-cycle fatigue tests at 538°C using strain rates of 4×10^{-4} , 1×10^{-2} and $5.2 \times 10^{-2} \text{ sec}^{-1}$ at strain ranges corresponding to fatigue life values of 200 and 2000 cycles as determined in (3) above;
 - 5) single low-cycle fatigue tests at 482° and 593°C using an axial strain rate of $2 \times 10^{-3} \text{ sec}^{-1}$ at strain ranges corresponding to fatigue life values of 200 and 2000 cycles as determined in (3) above;
- and 6) duplicate low-cycle fatigue tests at 538°C at a nominal axial strain rate of $2 \times 10^{-3} \text{ sec}^{-1}$ with a hold period of 300 seconds at peak tensile strain only and with a hold period of 300 seconds at peak compression strain only; the strain ranges employed should correspond to fatigue life values of 200 and 2000 cycles based on the continuous strain cycling evaluations in (3) above.

In these evaluations the room temperature tests were performed in air while all the elevated temperature tests were performed in high purity argon in which the oxygen level was maintained below 0.01 percent by volume.

All the tensile and fatigue tests were performed using hourglass-shaped specimens. A servo-controlled, hydraulically actuated fatigue testing machine was used in all these evaluations and the threaded test specimens were mounted in the holding fixtures of the test machine using special threaded adaptors. For the environmental (argon) tests a specially constructed pyrex containment vessel was positioned between the holding fixtures of the fatigue machine and neoprene low-force bellows at either end provided the seal to enable the desired gas purity levels to be maintained throughout the test. Side outlets (with appropriate seals) on this containment vessel provided entrance ports to accommodate the extensometer arms and similar side outlets provided entrance ports for the copper tubing leads to the induction coil. In addition, special ports near the bottom of the containment vessel enabled the thermocouples, used for specimen temperature measurement, to be routed out to the temperature control system. Specimen test temperatures were attained using induction heating and this was provided by positioning a specially designed induction coil around the test specimen (see Figure 1).

All force measurements were made using a load cell mounted within the loading train of the fatigue machine and specimen strains were measured by a specially designed, high temperature diametral extensometer. A special test procedure was developed to allow the short-term tensile tests to be performed at a constant strain rate which was maintained throughout the test. In the fatigue tests an analog strain computer was employed which allowed the diametral strain signal to be used in conjunction with the load signal so as to provide an instantaneous value for the axial strain which was then the controlled variable.

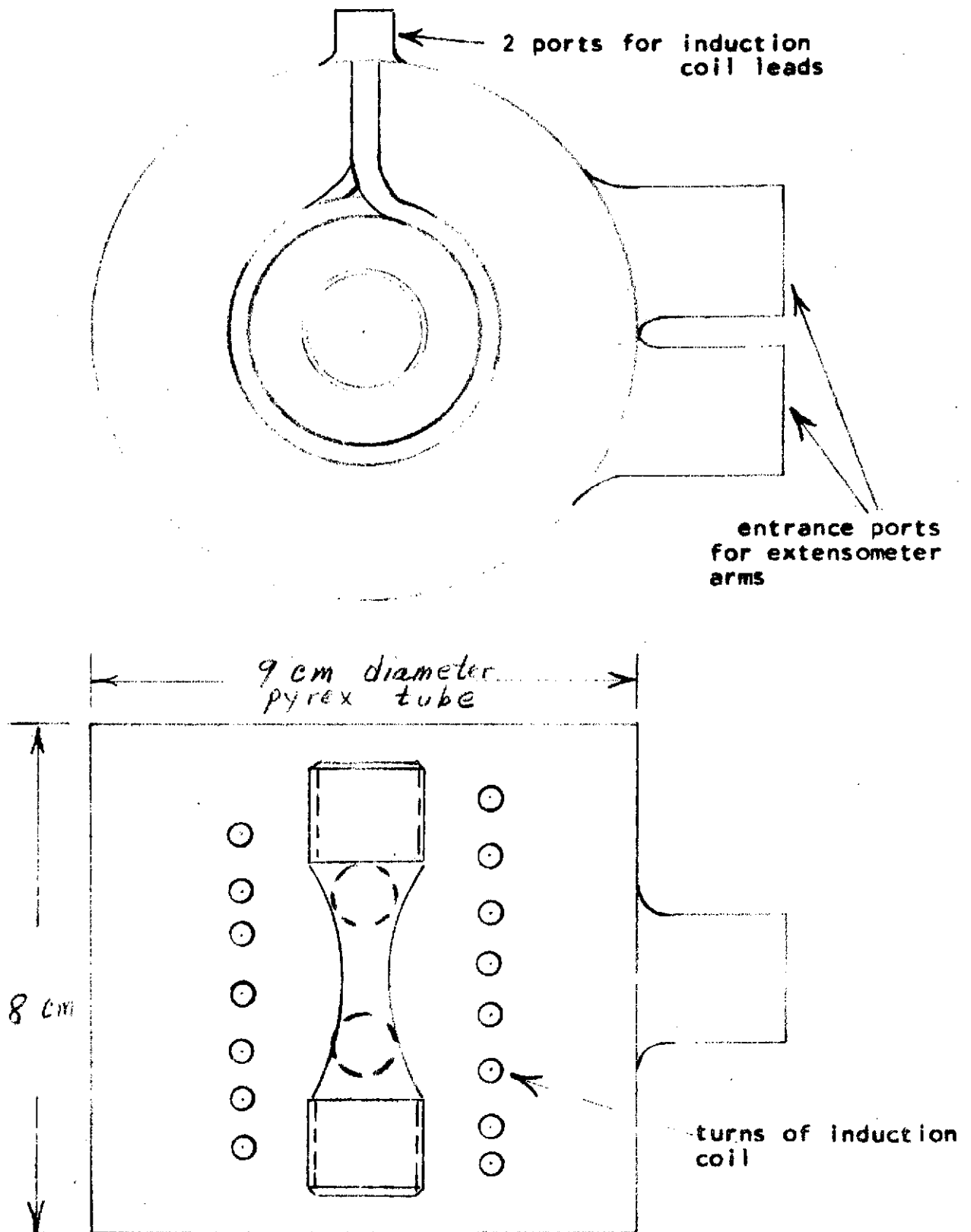


Figure 1- Schematic of Pyrex Environmental Chamber

III - MATERIAL AND SPECIMENS

Specimen material for use in this portion of the program was supplied by NASA-Lewis Research Center, Cleveland, Ohio. This material was the copper-base Narloy-Z alloy (designated R-24) developed by North American Rockwell and was furnished in the centrifugally cast form and had been hot-rolled, solution annealed and aged. Material was furnished in the form of plate stock 25 cm x 23 cm x 4 cm.

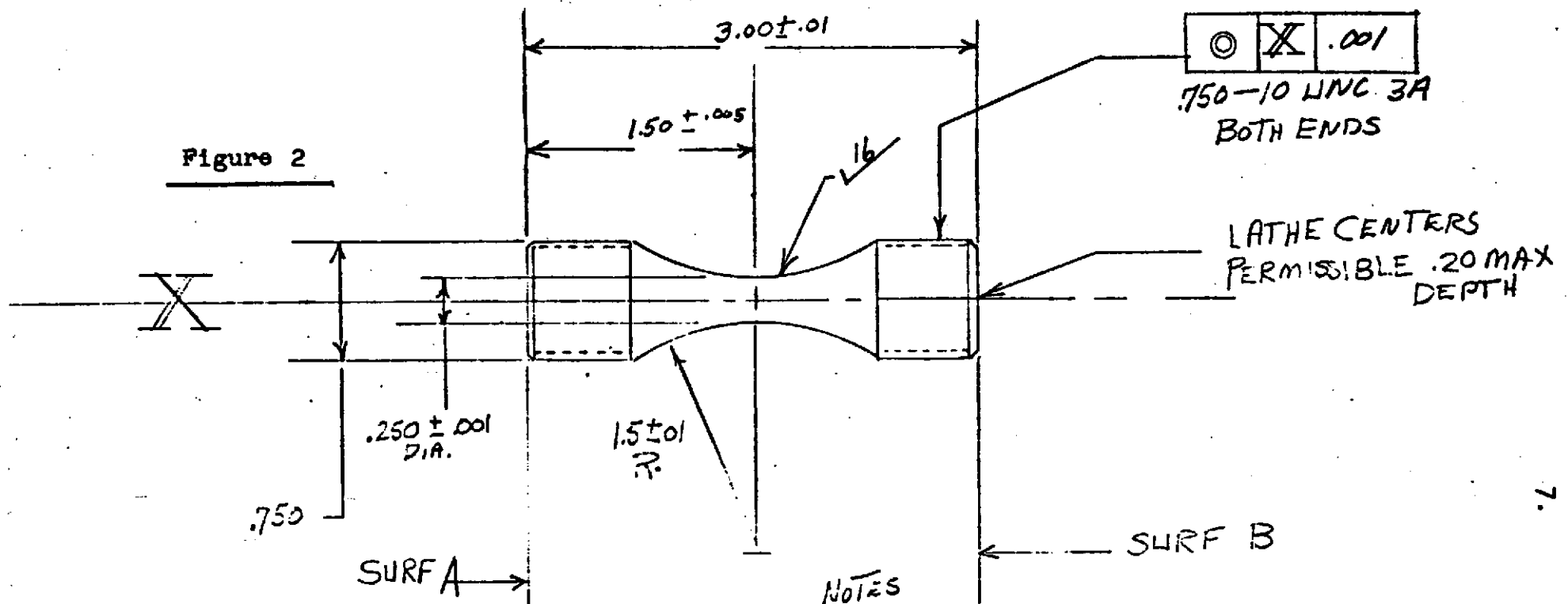
Using the specimen design shown in Figure 2, 48 specimens were fabricated from the R-24 plate. Forty two (42) of these were for use in the short-term tensile and fatigue evaluations while the remaining 6 specimens were retained as spares.

After being machined, all specimens were wrapped in soft tissue paper and placed in individual hard plastic cylinders (about 9 cm in length and 2.2 cm inside diameter). The ends of these cylinders were then sealed with masking tape and the specimen code number was written on the external surface of the cylinder. These cylinders were used for storage before and after test.

In preparing for a test each specimen was subjected to the following:

- 1) a small longitudinal notch was filed in the threaded sections of the specimen; this was designed to aid in the removal of entrapped air from the threaded area after the specimen was inserted in the adaptors (see below for specimen-adaptor assembly);
- 2) the specimen was washed with Freon to remove any surface oils which might have remained after machining;
- 3) a small quantity of dilute phosphoric acid was applied by hand to the complete surface of the specimen; this removed any surface oxides and any machining oil not removed by the cleaning with Freon; this operation was completed within 15 seconds;
- 4) the specimen was rinsed in warm water and dried using soft absorbent tissue;
- 5) the specimen was then subjected to a final cleaning with Freon.

Figure 2



5- SCREW THREADS TO BE AS LISTED IN NBS HANDBOOK H 28

NOTES

- 1- SURFACES A, & B TO BE PARALLEL WITHIN .001
- 2- SURFACES A, & B TO BE PERPENDICULAR TO CENTER LINE OF SPECIMEN WITHIN .0005 TIR
- 3- CONTOURED PORTION OF SPECIMEN TO HAVE A $\sqrt{16}$ FINISH OR BETTER. FINISHING SHOULD BE IN THE AXIAL DIRECTION USING LOW STRESS LAPPING OR POLISHING OPERATION
- 4- ALL DIMS TO BE CONCENTRIC WITHIN .001

UNLESS OTHERWISE SPECIFIED
DIMENSIONS ARE IN INCHES
TOLERANCES ON
FRACTIONS DECIMALS ANGLES
± ± ±

ALL SURFACES $\sqrt{16}$
MATERIAL
GOVT. OR COML. TO BE
SPECIFIED

DRAWN
DATE
APPD
ISSUED
APPROVED DATE
ENGR *STC* 1-12-71
MFG
MATL

SPECIMEN
Low CYCLE FATIGUE

Mar-Test inc.
CINCINNATI, OHIO

SIZE
MTI-1002

SCALE 1/1

WT CALS
ACTUAL

CONT ON SHEET SH NO.

IV - TEST EQUIPMENT

A closed-loop, servo-controlled, hydraulically-actuated fatigue machine (see Figure 3) was employed in this program. This machine was equipped with the necessary recorders to provide continuous readouts of the desired test information.

A block diagram of the type of test machine used is presented in Figure 4. The programmer is a precision solid-state device capable of furnishing all of the required waveform signals necessary to provide the strain or stress values demanded in the test. This signal is compared in the summing network with the strain or stress values actually present at the specimen at any instant of time. Any deviation from the required parameter is sensed by the servo-controller which supplies a correction current signal to the servo-valve which provides the correct hydraulic flow and pressure to the hydraulic actuator. The actuator in turn imparts the necessary displacement and force through the load cell to the specimen. The diametral displacement of the specimen in the gage section is sensed by the extensometer and the motion is imparted to the LVDT (Linear variable displacement transducer) which supplies an electrical signal to the analog computer. The analog computer accepts the instantaneous diametral strain and axial force signals and operates upon them to provide signals representing all of the strain and stress components of interest. Any one of these can be selected for comparison with the programmer signal.

Manufacturer and nomenclature of the various components of the fatigue machines are as follows:

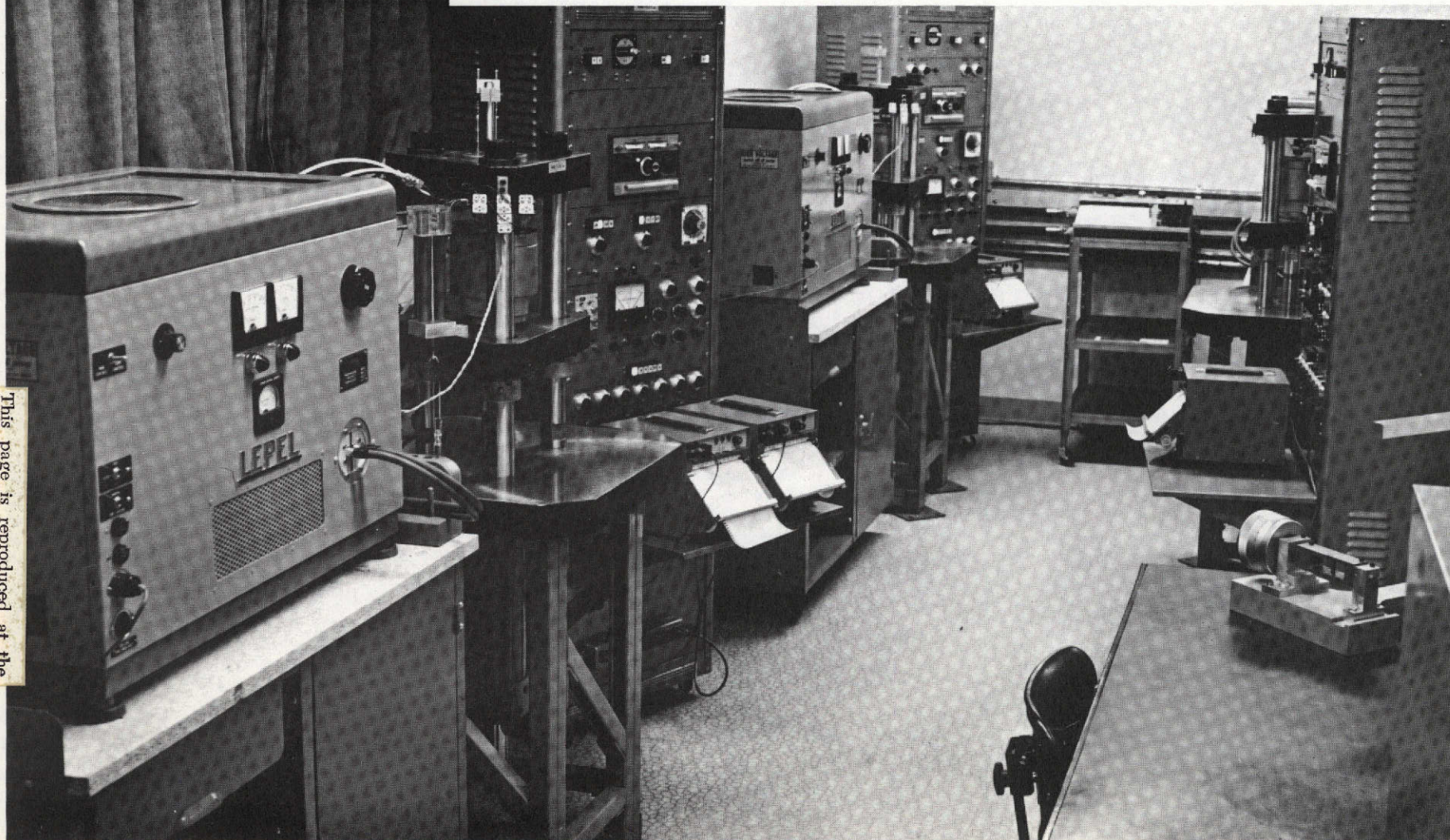
1. Programmer - designed and built by Mar-Test Inc.
2. Servo-controller - designed and built by Mar-Test Inc.
3. Actuator - Universal Fluid Dynamics, Type MDF5-H-BR
4. Servo-valve - Moog, Model 76-101
5. Hydraulic System - Racine, Model PSV-SSO-20GRS
6. Load Cell - Strainert, Model FFL15U-2SP (K)
7. Induction Generator - Lepel, Model T-2, 5-1-KC-J-BW
8. Extensometer - designed and built by Mar-Test Inc.
to measure diametral strain
9. LVDT - ATC, Model 6234A05801XX
10. Analog Strain Computer - designed and built by Mar-Test Inc.
11. Load Frame and Fixtures - designed and built by Mar-Test Inc.

Each fatigue machine consists of a sturdy three-column support system connecting two fixed, horizontal platens. A movable platen operates between the fixed platens and is hydraulically actuated to provide the desired cyclic motion. The movable platen contains three close-tolerance bushings which slide on the chrome-plated support columns to impart extreme rigidity and precise alignment to the system.

The diametral strain at the minimum diameter point of the specimen is measured using a specially constructed diametral extensometer. This device was fabricated from low thermal expansion materials (quartz and invar) to minimize the effects

Figure 3 Fatigue Laboratory at Mar-Test Inc.
Showing Three High Temperature Fatigue
Machines.

This page is reproduced at the
back of the report by a different
reproduction method to provide
better detail.



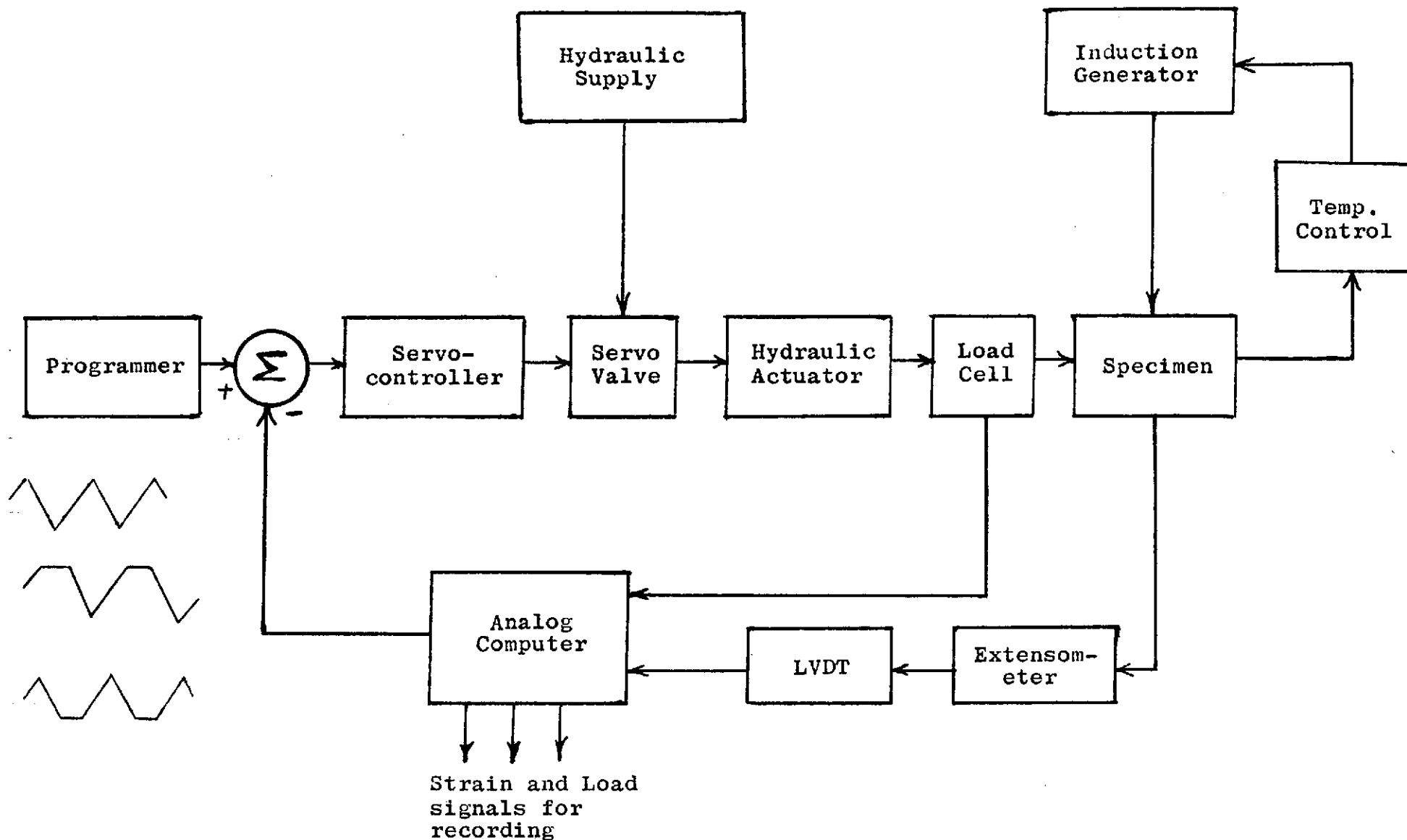


Figure 4. - Schematic of components in fatigue testing machine.

of room temperature changes on extensometer output. Each extensometer is calibrated prior to use by employing a special calibration fixture. Each device is supported horizontally (that is, in the actual use position) with the extensometer knife edges touching a 0.25 inch diameter split pin. One of the pin halves is fixed and the other is displaced horizontally to simulate a diameter increase. This motion is controlled by the rotation of the barrel of a special micrometer (calibrated against NBS standard). In this way the extensometer is calibrated to within 10 microinches. With this type of calibration and a knowledge of the stability and accuracy of the electronic components of the system a reasonable estimate of the accuracy of the strain control system is 60 microinches per inch in terms of axial strain range.

Before any tests are made each load cell is calibrated in position by placing a calibrated (NBS) Ring-Force Gauge (Morehouse Instrument Co., Model 5 BT, 5000 lbs capacity with an accuracy to 0.2 percent) in the specimen position in the load train. As the actuator is caused to apply a load the output of the load cell is plotted against the load indicated by the calibrated Ring-Force Gauge. This calibration is performed at frequent intervals to insure accurate stress measurements during the testing program.

Each fatigue machine has its own control console which functions to supply the very precise control features which are so essential to the performance of meaningful fatigue tests. In addition to housing the temperature controller and an elapsed time indicator each control console contains:

- a) a calibration panel which also provides means for automatic or manual control of the hydraulic solenoid and power for auxiliary equipment such as the induction generator and recorders;
- b) a programmer which provides the required demand signal waveform for the test;
- c) an analog strain computer which generates the load and strain components for recording and control purposes;
- d) a servo-controller which compares the programmer supplied demand signal and the computer supplied feedback signal and generates the proper control current for the servo-valve; a meter relay circuit operates in conjunction with the servo-controller to provide the means for shutting down the system when the specimen fails.

One of the important precautionary features of the Mar-Test fatigue machines is the incorporation of a manually operated by-pass valve across the hydraulic actuator. With this valve open the test specimen cannot be exposed to any inadvertent load transients during start-up. The hydraulic solenoid valve can be energized with this valve open and the load transients frequently encountered in test start-up can be eliminated. Once

the solenoid valve is opened the by-pass valve can be closed slowly to bring the system under control. During this operation the load trace is monitored so that a smooth transfer is effected and all load transients are eliminated.

V - TEST PROCEDURES

A. Low-Cycle Fatigue

The closed-loop, servo-controlled low-cycle fatigue machine employed in this study was fitted with a specially constructed containment vessel to allow testing in a protective environment. This cylindrical chamber was fabricated from 9-cm diameter pyrex tubing and was inserted between the holding fixtures. This small-volume enclosure (about 500 cm³) facilitated system purging and allowed the desired protective gas purity levels to be maintained. Neoprene low-force bellows at the top and bottom connected the chamber to the holding fixtures and permitted the normal longitudinal motion of the specimen during cyclic loading. Side-arms on the pyrex containment vessel provided access for the extensometer arms and a special flexible joint provided an effective seal without influencing the strain measurement. Similar side-arms provided access for the copper tubing leads for the induction coil. In addition, ports were provided near the lower platen so that the thermocouple leads could be routed from within the enclosure to the temperature control system. Specimen heating was effected by means of a specially wound induction coil which was positioned to enclose the test specimen (see Figure 1).

All the low-cycle fatigue tests in this program were performed using the specimen configuration shown in Figure 2. Such specimens were held in specially designed threaded adaptors to provide an integral assembly that allowed the adaptor to be heated inductively along with the specimen itself. Large mating surfaces were provided between the specimen and the adaptors to minimize the temperature gradient between them. This approach proved to be quite successful and test temperatures to 593°C (1100°F) were achieved quite readily. It was also shown that a very flat longitudinal temperature profile was obtained.

Test temperatures were measured using a chromel-alumel thermocouple clamped tightly against the specimen in the region where the contoured portion of the specimen meets the threaded portion. This approach was found to be very reliable and very easy to apply.

Because of the temperature uniformity in the specimen-adaptor assembly a special precaution must be taken to avoid failure in the threaded portion of the specimen. This involves the provision of a large specimen diameter in the grip region compared to the diameter at the specimen midpoint. This was also sufficient to avoid plastic deformation at the specimen-adaptor contact point and therefore to prevent backlash and alignment changes during strain cycling.

A fully instrumented test specimen-adaptor assembly was mounted in the holding fixture of the fatigue machine using

a split collet type of assembly and a special leveling device was employed to assure that the specimen was installed perpendicular to the platens. A flat load cell (see previous section) in series with the specimen was used to measure the load applied to the specimen throughout the test.

Once the specimen was installed within the containment vessel the system was purged using a high flow rate of high purity argon (see below for inert gas specifications) for 30 minutes. This established the desired purity level within the test chamber. The inert gas flow rate was then lowered to a few cm³/min and maintained at this level throughout the test.

Before any tests were initiated the analog strain computer was calibrated by making use of the specimen cross-sectional area (A) and the value for Young's modulus (E) at the intended test temperature. Modulus values for the two alloys tested were determined in separate tests. The values of A and E were used as shown in the block diagram in Figure 5 to generate axial strain values corresponding to measured values of diametral strain and force. This diagram provides an aid to an understanding of the computer calibration procedure which is based on using the values of A and E and adjusting the compliance control to establish the following equality:

$$A E = F / \epsilon_e$$

Prior to heating a specimen to the desired test temperature the system was placed in force control. This automatically kept the force at zero by gradually lowering the movable platen to account for the thermal expansion of the specimen as the temperature was increased. When test temperature was obtained the analog strain computer was employed to yield a value for Poisson's ratio. The specimen was cycled elastically so that the actual plastic strain, $\Delta \epsilon_p$ was zero and the value of Poisson's ratio could be obtained by the ratio of the diametral to axial strain; thus:

$$\nu_e = \frac{-\epsilon_d}{\epsilon_e}$$

The ν_e control on the computer was then adjusted to force the computer value of $\Delta \epsilon_p$ to zero. At this point the above relations were satisfied and the correct value of ν_e was indicated on a potentiometer turns-counting dial on the computer panel (the value for Poisson's ratio, plastic, was set internally to 0.5 in accordance with constant volume deformation conditions associated with plastic deformation). At this point the computer was calibrated and furnished a correct axial strain signal for recording and control purposes.

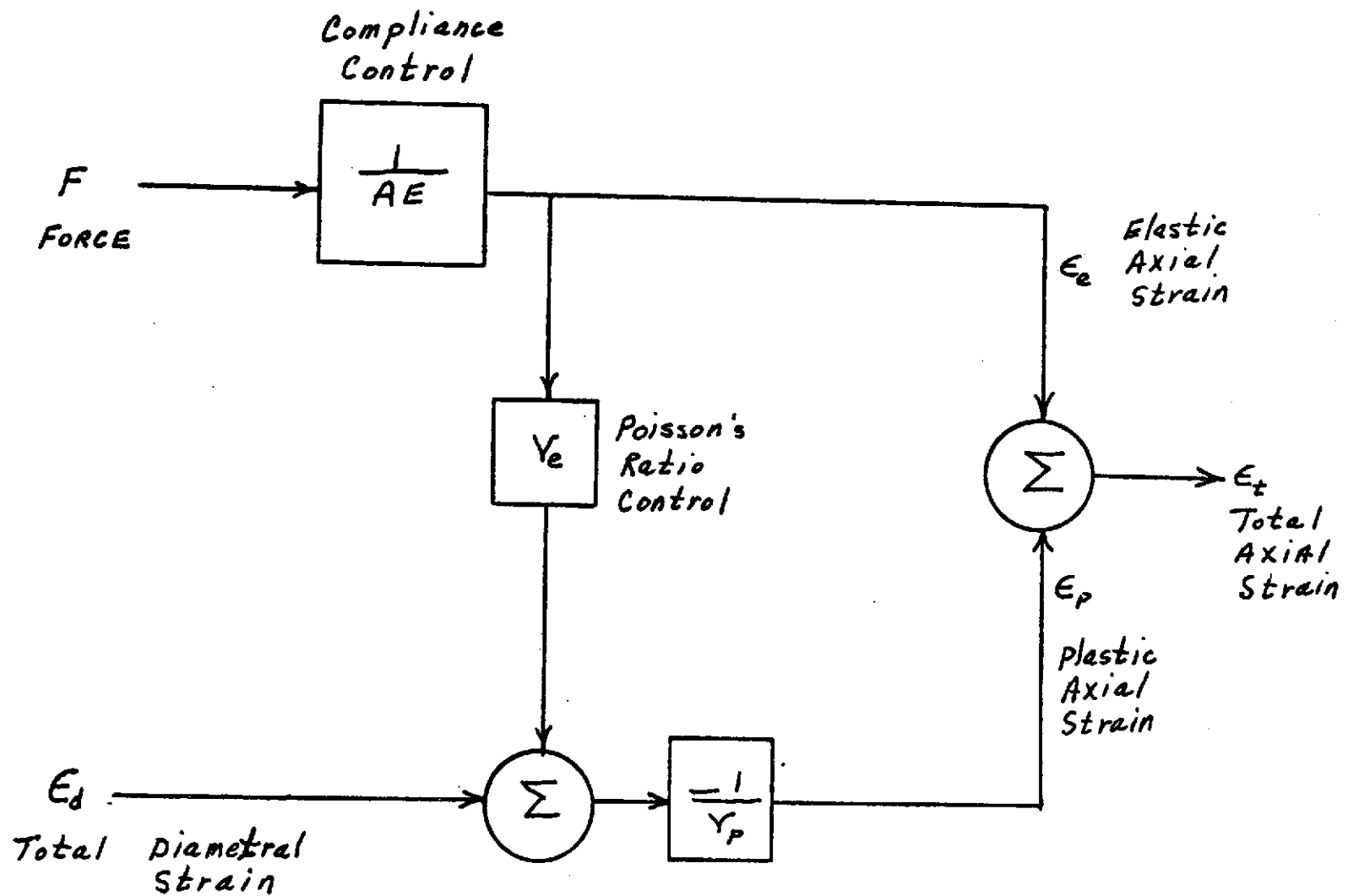


Figure 5 - Block Diagram of Strain Computer

With the computer calibration complete the test was ready to begin. Two recorders were connected to the console, one to monitor load and the other to monitor the total axial strain. The system was placed in automatic control and the strain was gradually increased to the desired level. This gradual increase to the desired strain level requires 5 or 6 cycles and avoids specimen damage due to "overshooting" the strain range which can occur if an attempt is made to impose the desired strain level on the first loading cycle. When the desired strain range was reached the test conditions were kept constant until fracture occurred. Hysteresis loops were recorded on an x-y recorder during the first few cycles and at frequent intervals thereafter. In addition, a continuous recording was made of the applied load and the associated plastic strain. When the specimen fractured, the shut-down circuit automatically de-energized the entire testing system including the induction generator, the hydraulic ram, the timing device and the recorders. However, the protective environment system remained functional until the specimen cooled to room temperature.

High purity (guaranteed 99.999% purity or better) argon gas with 1000 ppm of hydrogen added was employed as the protective environment for the elevated temperature tests. This same environment was employed in the previous elevated temperature evaluations (see NASA CR-121260 and CR-121261) of copper-base alloys and proved to provide satisfactory results for all the high temperature tests performed in this program.

B. Short-Term Tensile

Measurements of short-term tensile behavior were made using the same hydraulically-actuated, servo-controlled fatigue machines employed in the low-cycle fatigue evaluations. Furthermore, the same specimen design was employed and the specimen preparation, test environment, installation and instrumentation procedures were identical to those employed in the fatigue tests. These short-term tensile tests were performed using a diametral extensometer and the true diametral strain rate was kept constant at the specified value (the corresponding axial strain rate was about twice this value).

For each test a strip chart recording was made of the measured diametral strain as a function of time and, in addition, an x-y recording was made of the load versus diametral strain. These traces provide test information from the instant of load application all the way to fracture.

VI - TEST RESULTS AND DISCUSSION OF RESULTS

A) Short-Term Tensile

Short-term tensile tests of the R-24 alloy were performed in duplicate at room temperature, 482°O, 538°O and 593°O using an axial strain rate of $2 \times 10^{-3} \text{ sec}^{-1}$. In addition, duplicate tests were performed at 538°O using strain rates of 1×10^{-2} and $4 \times 10^{-4} \text{ sec}^{-1}$. The room temperature tests were performed in air while all the elevated temperature tests were performed in high purity argon.

A summary of the test results obtained in these short-term tensile evaluations is presented in Table 1. A plot of the effect of temperature on tensile properties is presented in Figure 6. The behavior pattern for ultimate and yield strength follows that exhibited by the zirconium-copper alloys (R-2 and R-20) studied previously (see NASA CR-121261). In terms of ultimate tensile strength the behavior of the R-24 alloy is essentially identical to that of the R-20 alloy but noticeably less than that of the R-2 alloy, all tested at the same strain rate. In terms of room temperature yield strength the value for the R-24 alloy is much lower than that exhibited by the R-2 and R-20 compositions; in the elevated temperature regime the yield behavior of the R-24 alloy is essentially the same as that of the R-20 composition but still much below that of the R-2 alloy.

A minimum ductility point appears to be indicated in the R-24 results at a strain rate of $2 \times 10^{-3} \text{ sec}^{-1}$. These reduction in area values of 40 to 50% are much lower than the 80 to 90% values obtained for the R-2 and R-20 compositions tested at the same temperatures and strain rates.

An illustration of the effect of strain rate on the tensile properties of the R-24 alloy is shown in Figure 7. The most significant effect is the noticeable increase in reduction in area values as the strain rate is increased.

B) Low-Cycle Fatigue

1) Continuous Cycling Behavior at 538°O and a Strain Rate of $2 \times 10^{-3} \text{ sec}^{-1}$

A series of low-cycle fatigue tests of the R-24 alloy was performed at 538°O in high purity argon using a strain rate of $2 \times 10^{-3} \text{ sec}^{-1}$. A summary of the results obtained in these tests is presented in Table 2. In addition to reporting the number of cycles to failure the value for N_5 (the number of cycles corresponding to a 5% reduction in tensile load from the steady state value) is also included. Due to the continual cyclic softening (after a slight hardening in the first few cycles) that was exhibited in these tests (see Figure 8a), no stable or steady state load level was attained for use as a basis for the N_5 determination. For this reason the N_5 value had to be selected in a different fashion. An analysis of the load versus cycles record obtained in each test

Table 1 - Short-Term Tensile Properties of R-24 (Narloy Z) Alloy Measured in Argon
(Room Temperature Tests Were Performed in Air).

Diametral Extensometer			Hourglass-Shaped Specimens		
Spec. No.	Temp., °C	Strain Rate, sec ⁻¹	0.2% Offset Yield Strength, MN/m ²	Ultimate Tensile Strength, MN/m ²	Reduction in Area, %
R-24-1	RT	2×10^{-3}	196.5	316.5	51
R-24-2	RT	2×10^{-3}	200	315.8	51
R-24-3	482	"	149.6	182	50
R-24-4	482	"	148	177	48
R-24-5	538	"	131	153	41
R-24-6	538	"	129	152.4	42
R-24-7	593	"	102.7	114.5	48
R-24-8	593	"	110.3	121.4	45
R-24-9	538	1×10^{-2}	130.3	163.4	51
R-24-10	538	1×10^{-2}	132.4	168.9	51
R-24-11	538	4×10^{-4}	122	134.4	36
R-24-12	538	4×10^{-4}	124	134.4	33

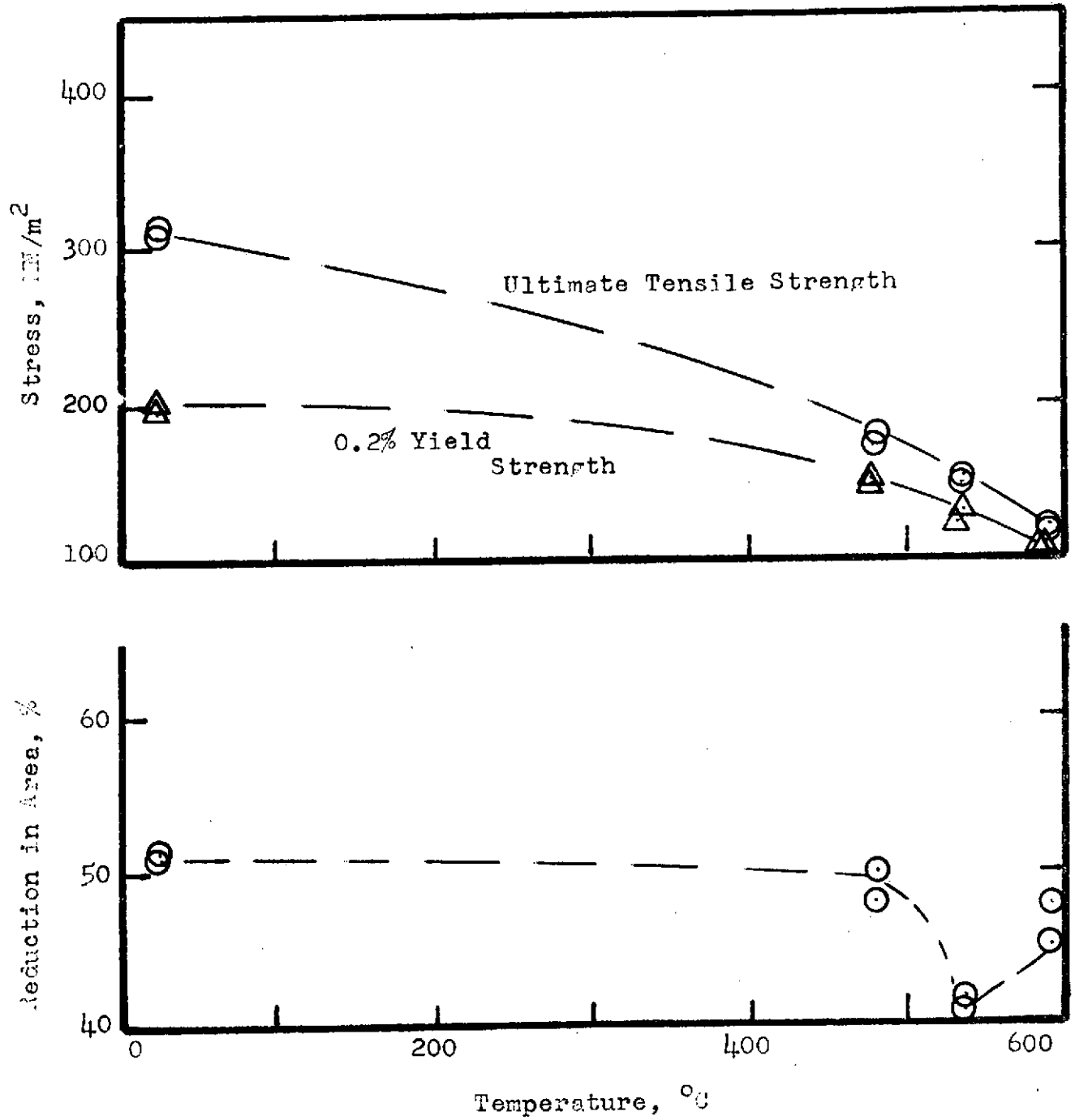


Figure 6 - Tensile properties of R-24 alloy as a function of temperature at a strain rate of $2 \times 10^{-3} \text{ sec}^{-1}$.

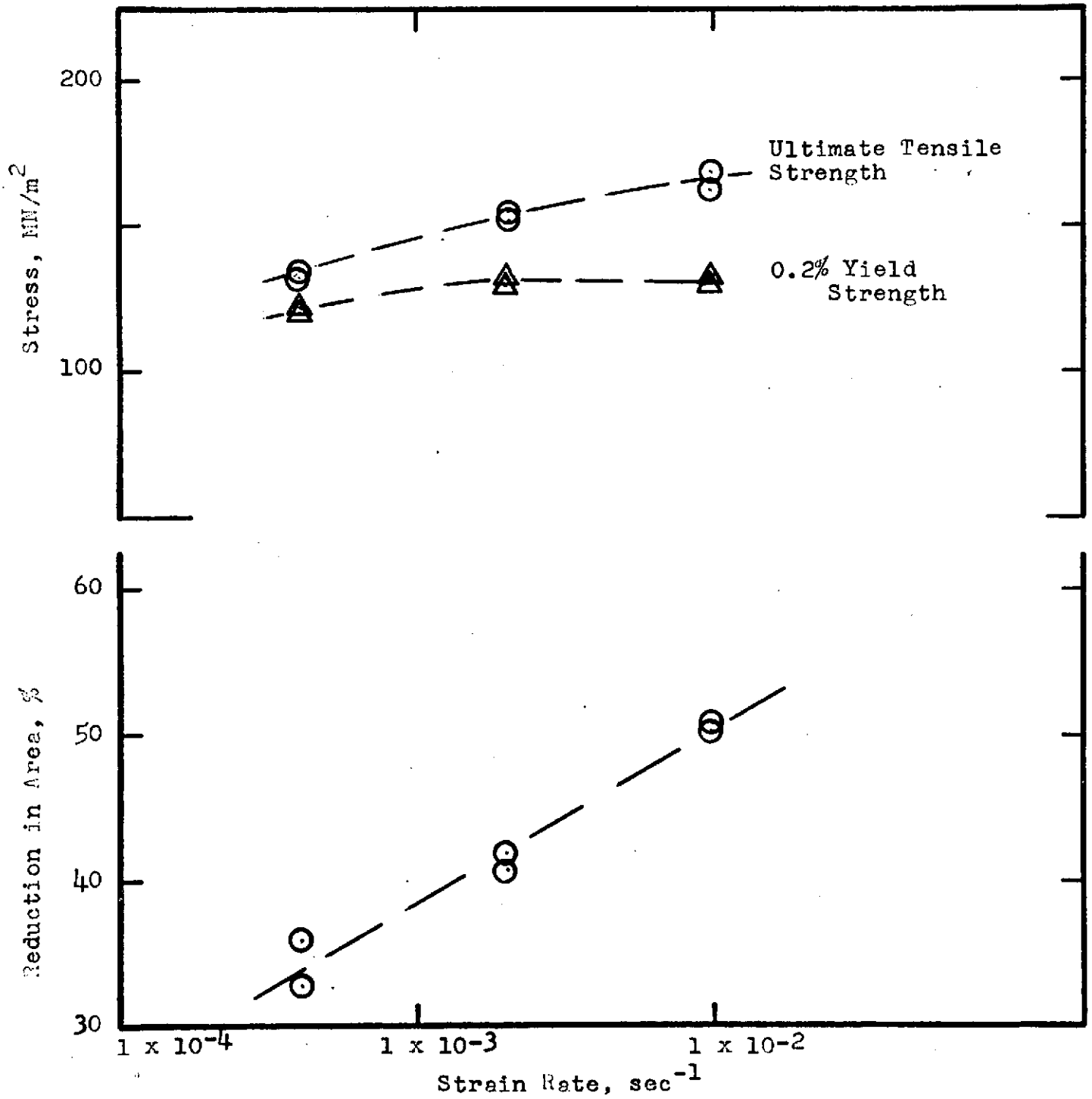


Figure 7 - Tensile properties of R-24 alloy at 538°C as a function of strain rate.

Table 2- Low-Cycle Fatigue Test Results Obtained in Argon at 538°C Using a Strain Rate of $2 \times 10^{-3} \text{ sec}^{-1}$.

R-24 Series
Narloy Z (cent. cast, hot-rolled, solution annealed and aged)

Axial Strain Control
A - ratio of infinity

$$E = 98.6 \times 10^3 \text{ MN/m}^2$$

Spec. No.	Poisson's Ratio	Total Strain Range, %	Freq. cpm	Stress Range at Start, MN/m ²	at $N_f/2$			N_f , Cycles to Failure	N_5 , cycles (see text for definition)
					ΔE_p %	ΔE_e %	$\Delta \sigma$ MN/m ²		
R-24-13	0.345	1.0	6	272	0.752	0.248	245	1,169	1140
R-24-14	0.335	2.0	3	300	1.717	0.283	279	331	274
R-24-15	0.335	1.2	5	283	0.948	0.252	248	1,126	926
R-24-16	0.34	0.7	8.57	265	0.476	0.224	220	3,601	3000
R-24-17	0.34	3.5	1.714	307	3.203	0.297	293	99	87
R-24-18	0.34	2.5	2.4	300	2.22	0.280	276	253	220
R-24-19	0.34	0.85	7.06	269	0.62	0.23	228	2469	2000
Notes: all specimens exhibited a slight initial cyclic hardening followed by cyclic softening									

identified a regime within which the tensile load decreased linearly with the number of cycles. At a certain point (designated N^* in this analysis) the load begins to decrease at a rate greater than that noted in the linear regime. The load at the N^* point was then noted and N_5 was selected as the number of cycles at which the tensile load attained a value which was 5% lower than the tensile load at the N^* point.

A logarithmic plot of the strain range versus N_f and N_5 for the R-24 alloy is shown in Figure 8b. It will be noted that the N_5 values are consistently about 0.82 of the N_f values over the entire strain range regime studied. A similar plot would be obtained if the N^* values were employed for it was noted that the ratio of N^* to N_5 was always about 0.90.

In another analysis of these tests the hysteresis loops were employed to provide an indication of crack initiation. For this type of cycling the presence of a crack leads to the formation of a cusp near the compression tip of the hysteresis loop. This behavior is illustrated in Figure 9 using two hysteresis loops from the test of Spec. R-24-17. While the cusp is well-developed in this illustration the very first indication of a point of inflection in the compression portion of the hysteresis loop can be assumed to represent the crack initiation point, N_i . When this interpretation was employed the points shown in Figure 8b were obtained to indicate that the N_i point occurs just slightly before half-life over the entire strain range regime employed in these tests.

A plot of the elastic and plastic strain ranges versus N_f for the data presented in Table 2 is shown in Figure 10. The linearities defined in this plot correspond to slopes of -0.09 and -0.60 for the elastic and plastic strain ranges respectively.

2) Strain-Rate Effects at 538°C

The effect of strain rate on the low-cycle fatigue behavior of the R-24 alloy at 538°C was studied using strain rates of 4×10^{-4} , 1×10^{-2} and $5.2 \times 10^{-2} \text{ sec}^{-1}$. A summary of the test results is shown in Tables 3 and 4 and the fatigue life is plotted as a function of strain range in Figure 11. A comparison of these data with similar results obtained for the R-24 alloy at a strain rate of $2 \times 10^{-3} \text{ sec}^{-1}$ (see Figure 8b) indicates a definite increase in the fatigue life as the strain rate is increased. A plot defining the effect of strain rate on the fatigue life of the R-24 alloy at strain ranges of 0.9 and 2.6% at 538°C is shown in Figure 12. Two tests of the zirconium-copper, R-2, alloy (see NASA CR-121260 for composition and supporting data) were also performed (see Table 4) at a strain range of 2.6% and a strain rate of $5.2 \times 10^{-2} \text{ sec}^{-1}$ and these data points are shown in Figure 12 for comparison with the R-24 results. It is interesting that the R-24 data at a strain range of 2.6% suggest a definite saturation effect in both the high and low strain rate regimes. This is completely consistent with the behavior pattern to be expected based on the concept of strain range.

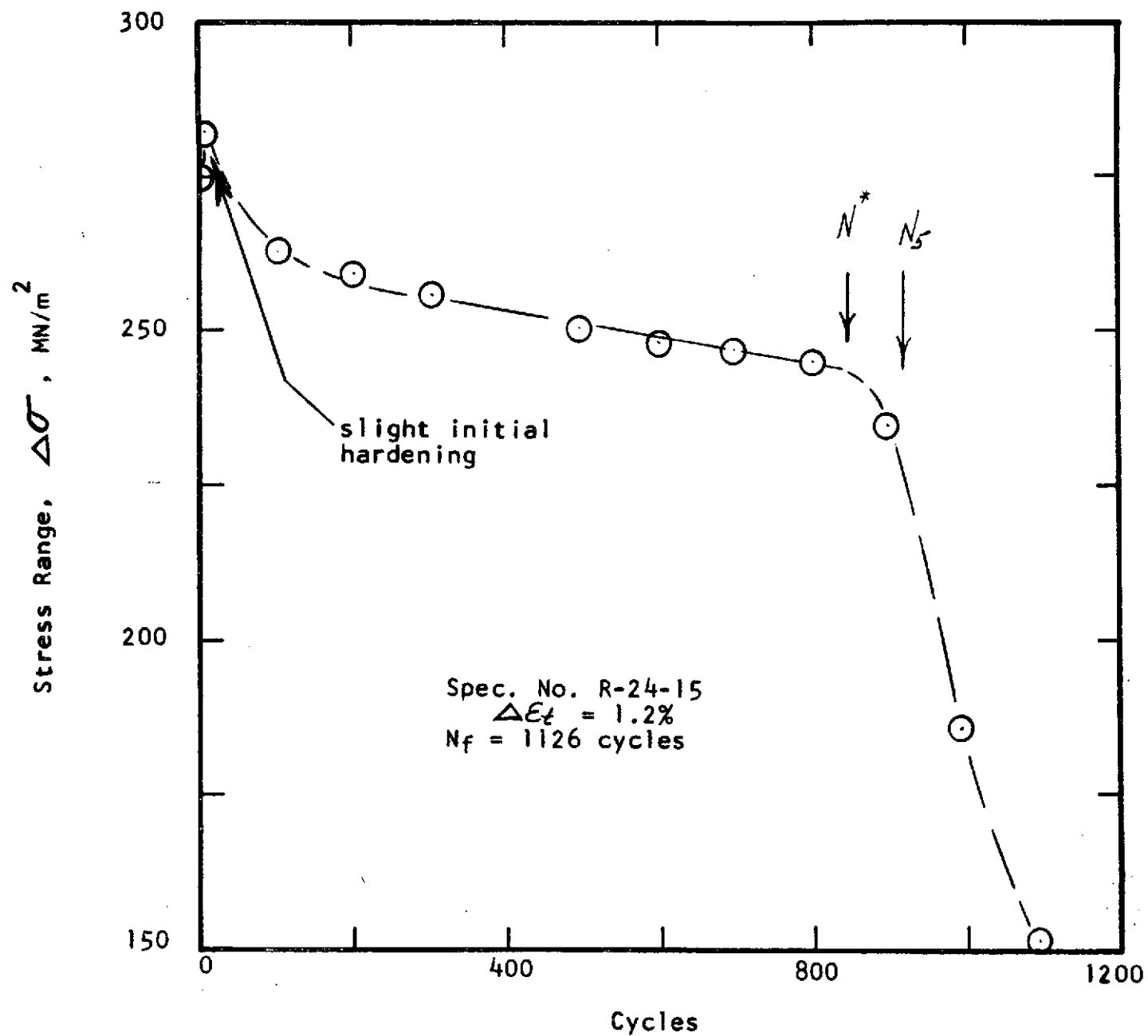
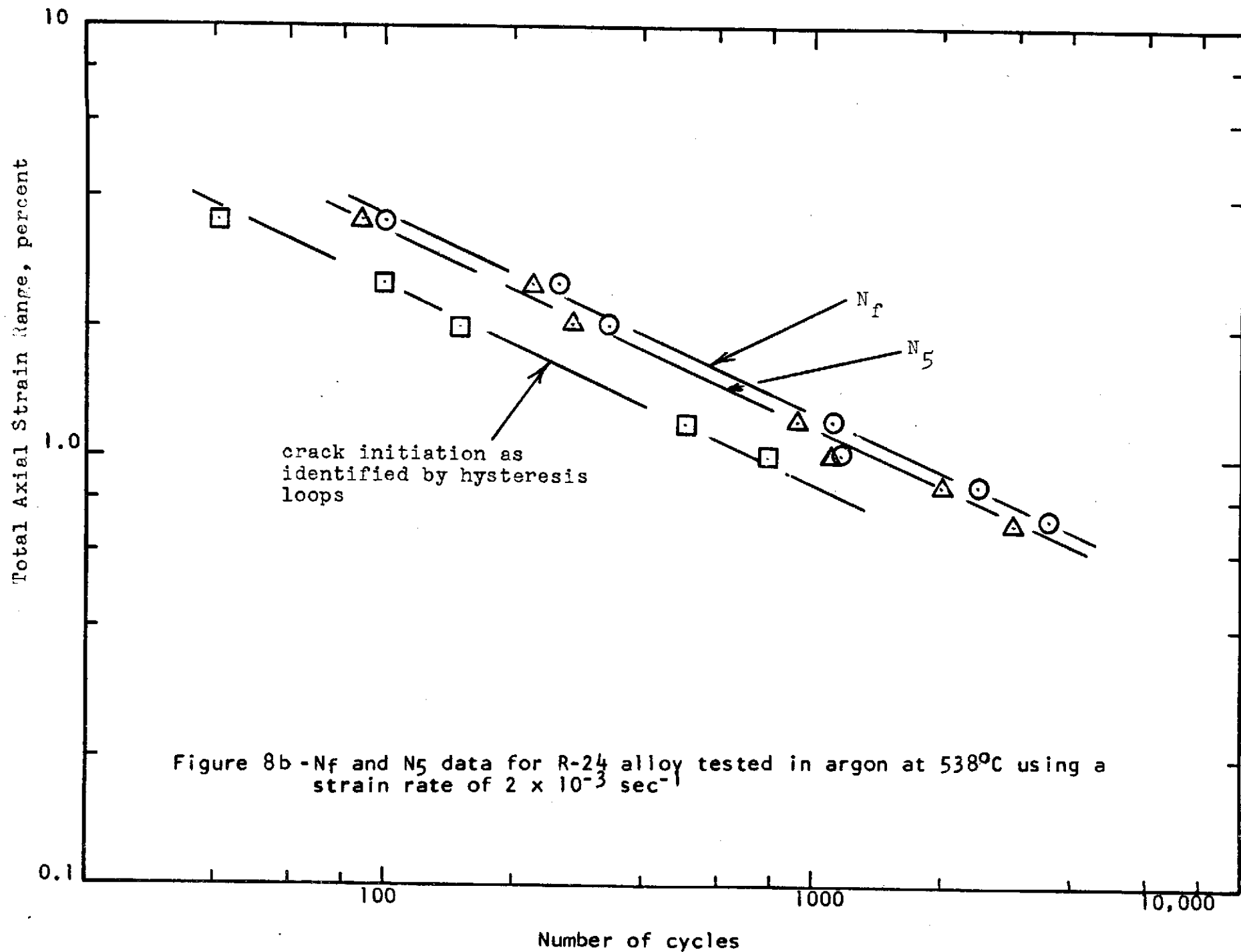


Figure 8a - Example of Cyclic Strain Softening in R-24 alloy tested in argon at 538°C using a strain rate of $2 \times 10^{-3} \text{ sec}^{-1}$.



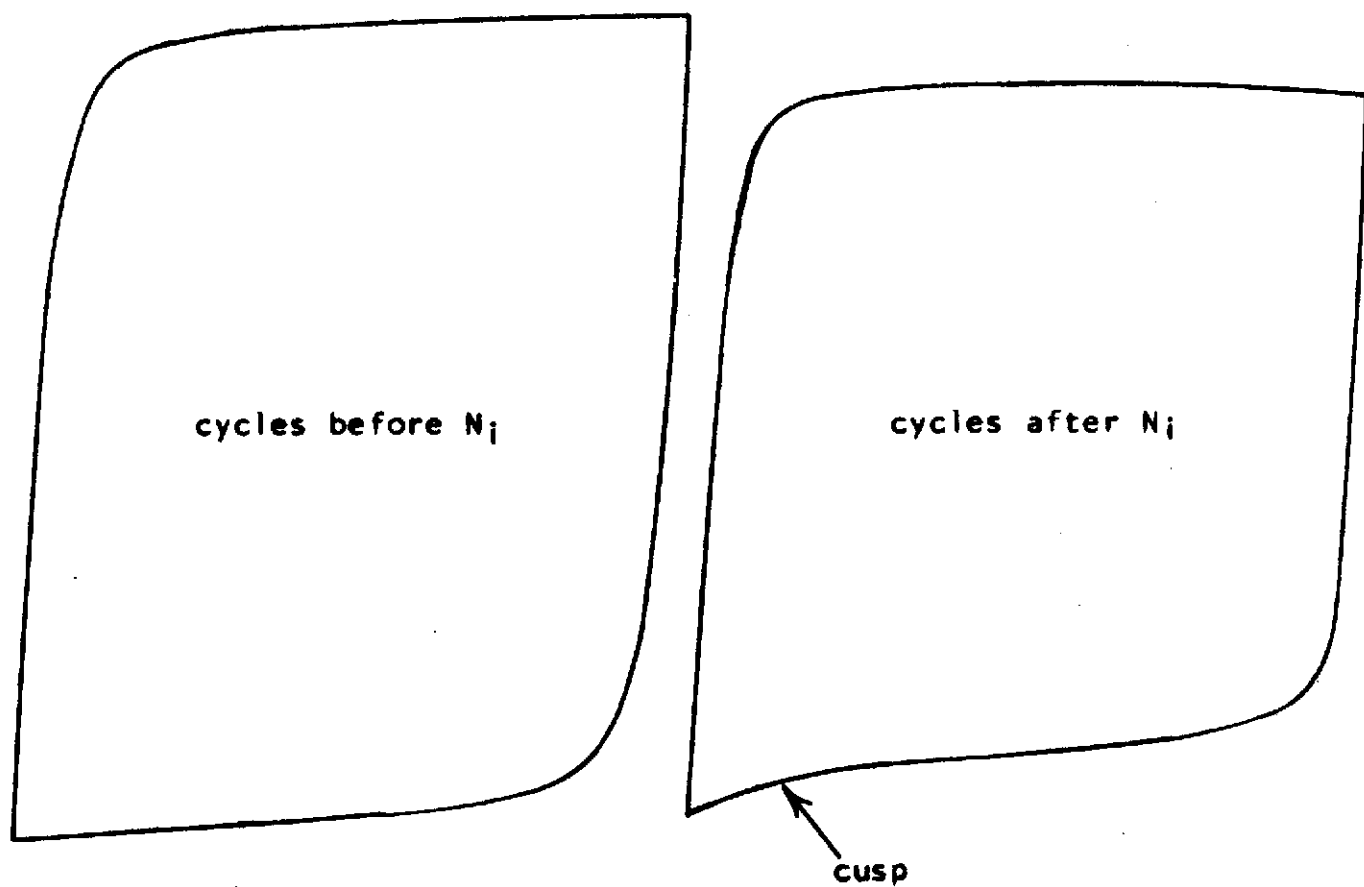


Figure 9- Hysteresis loops obtained for Spec. R-24-17 showing formation of cusp to indicate the presence of a crack.

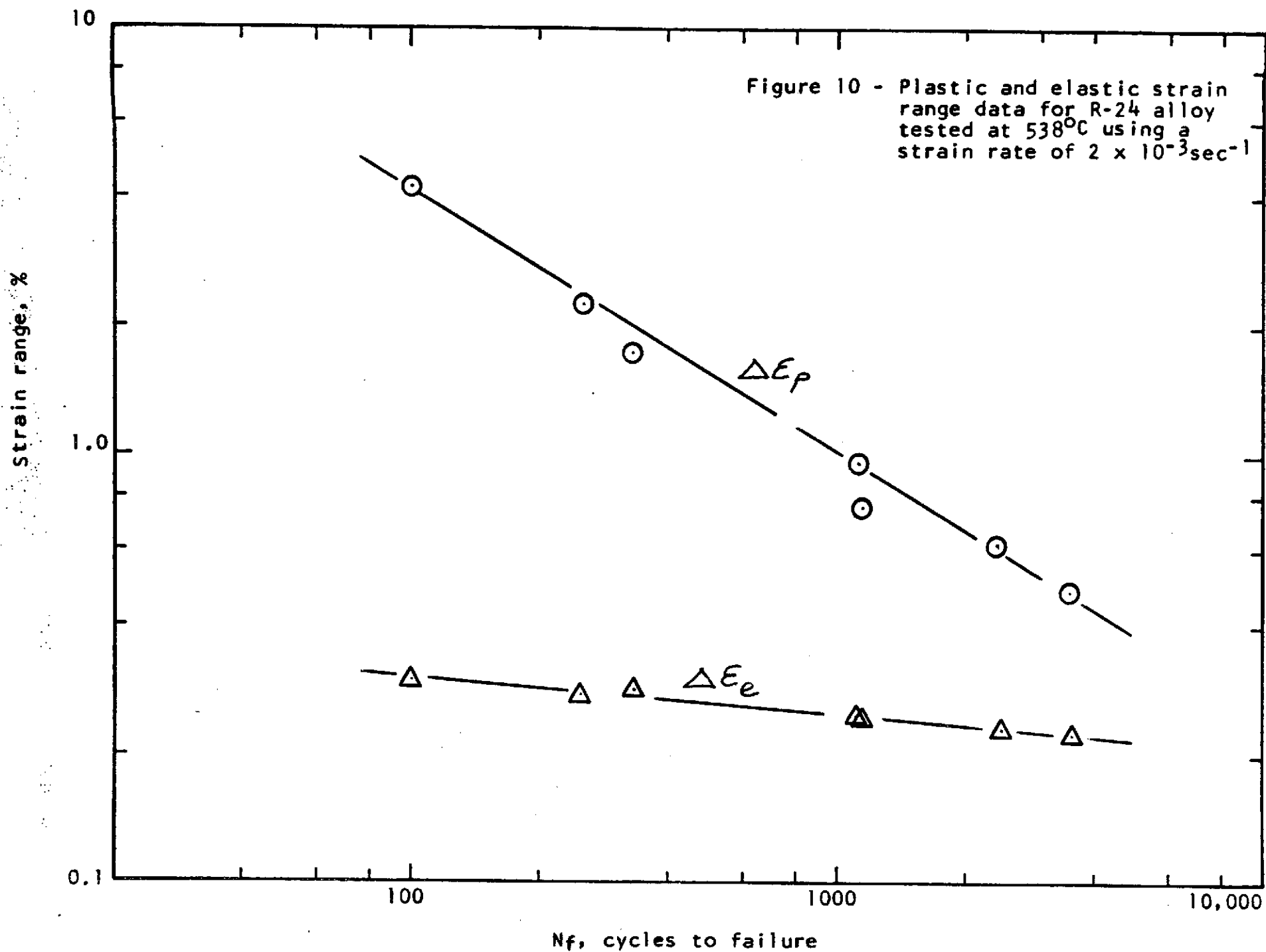


Table 3 - Low-Cycle Fatigue Test Results Obtained in Argon at 538°C for Strain Rates of 4×10^{-4} and $1 \times 10^{-2} \text{ sec}^{-1}$.

R-24 Series Narloy Z (cent. cast, hot-rolled, solution annealed and aged)					Axial Strain Control A - ratio of infinity E = $98.6 \times 10^3 \text{ MN/m}^2$				
Spec. No.	Poisson's Ratio	Total Strain Range, %	Freq. cpm	Stress Range at Start, MN/m^2	at $N_f/2$			N_f , Cycles to Failure	N_5 , cycles (see text for definition)
					$\Delta \epsilon_p$ %	$\Delta \epsilon_e$ %	$\Delta \sigma$ MN/m^2		
					<u>$1 \times 10^{-2} \text{ sec}^{-1}$</u> (see Note A)				
R-24-22	0.335	0.9	33.3	276	0.641	0.259	255	3,909	3000.
R-24-21	0.34	0.9	33.3	276	0.641	0.259	255	3,586	3350
R-24-23	0.34	2.6	11.54	310	2.272	0.328	325	339	300
R-24-26	0.34	2.6	11.54	314	2.272	0.328	325	364	340
					<u>$4 \times 10^{-4} \text{ sec}^{-1}$</u> (see Note B)				
R-24-20	0.34	0.9	1.33	265	0.69	0.21	207	1,138	980
R-24-25	0.34	0.9	1.33	255	0.69	0.21	207	1,196	1010
R-24-24	0.34	2.6	0.46	276	2.348	0.252	248	154	115
R-24-27	0.34	2.6	0.46	269	2.359	0.241	238	133	115
A) all specimens exhibited a slight initial cyclic hardening followed by cyclic softening									
B) all specimens exhibited cyclic softening									

Table 4 - Low-Cycle Fatigue Results Obtained in Argon at 538°C Using a Strain Rate of $5.2 \times 10^{-2} \text{ sec}^{-1}$

R-2 (zirconium-copper, 1/2 Hard) alloy
and
R-24 (Narloy Z) alloy

Axial Strain Control
A-ratio of infinity

Spec. No.	Poisson's Ratio	Total Strain Range, %	Freq. cpm	Stress Range at Start, MN/m ²	at $N_f/2$			N_f , Cycles to Failure	N_5 , cycles (see text)
					$\Delta \epsilon_p$, %	$\Delta \epsilon_e$, %	$\Delta \sigma$, MN/m ²		
R-24-29	0.34	2.6	60	372	2.22	0.38	372	474 ^a	--
R-24-30	0.34	2.6	60	374	2.22	0.38	374	588 ^a	570
R-2-74	0.35	2.6	60	303	2.38	0.22	179	3,132 ^b	3000
R-2-75	0.35	2.6	60	282	2.39	0.21	167	3,480 ^b	3350

a) stable

b) cyclic softening

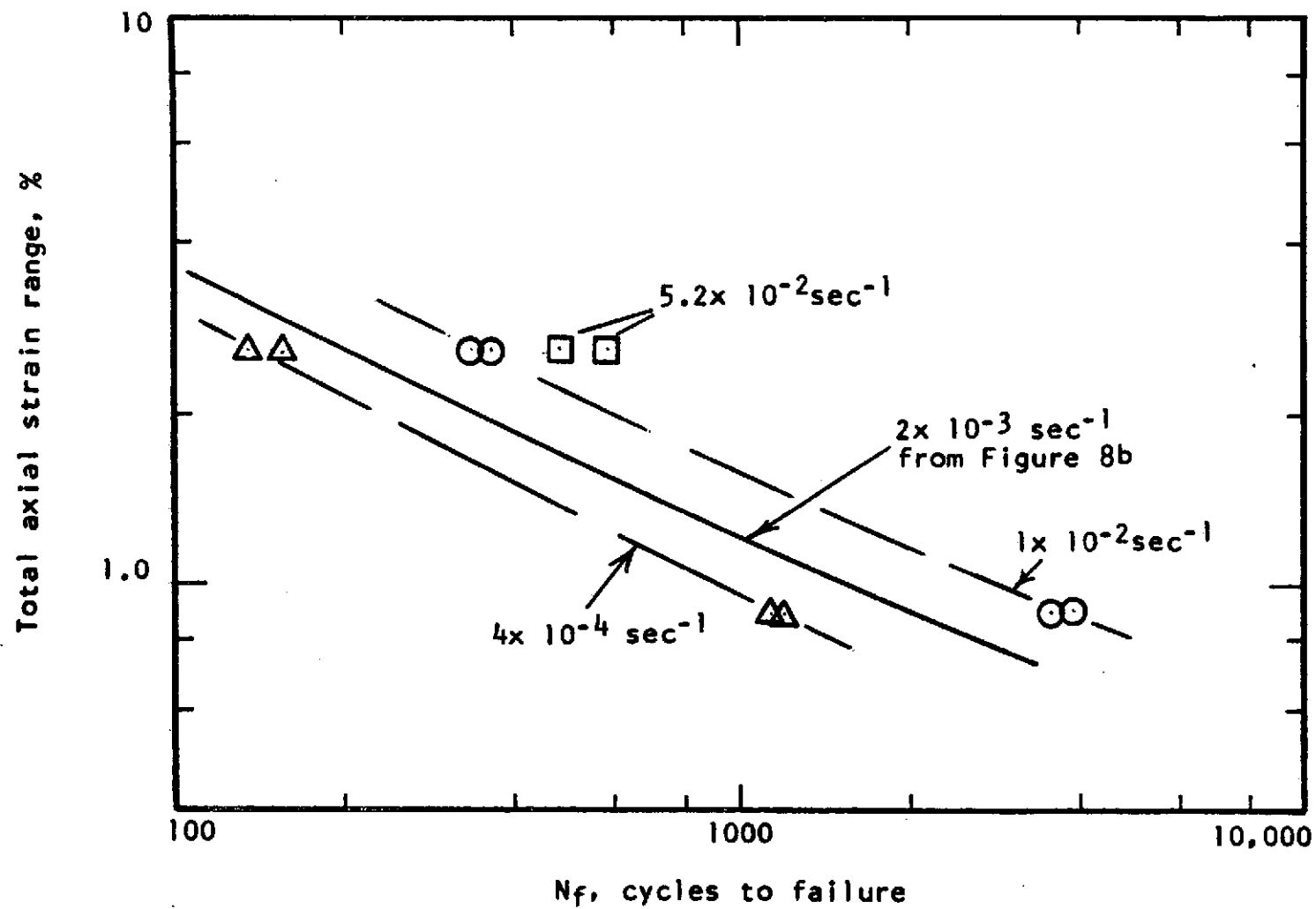


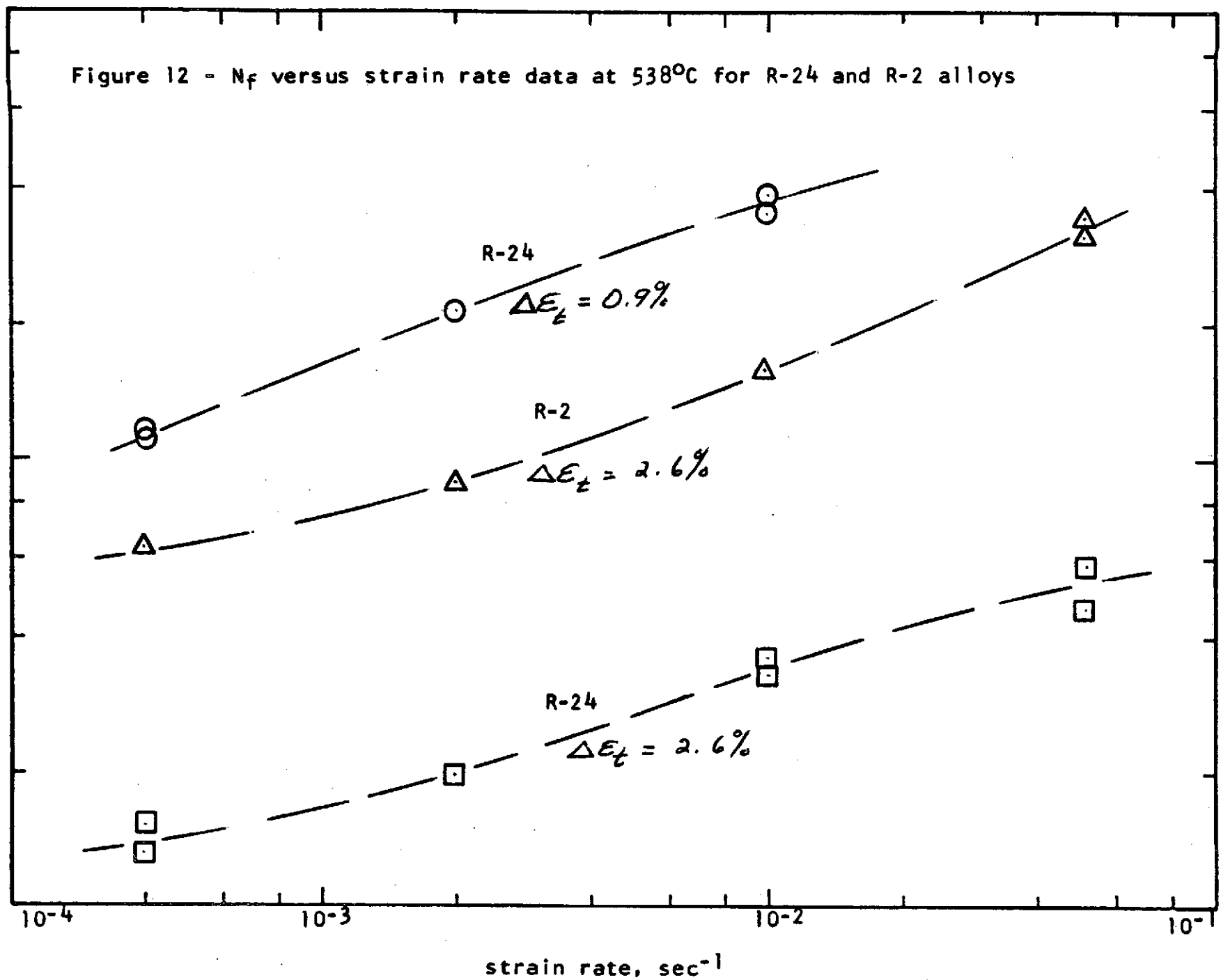
Figure 11 - Effect of strain rate on fatigue life of R-24 alloy tested in argon at 538°C

10,000

Figure 12 - N_f versus strain rate data at 538°C for R-24 and R-2 alloys N_f , cycles to failure

1000

100

strain rate, sec^{-1}

30.

partitioning (see S. S. Manson, "The Challenge to Unify Treatment of High Temperature Fatigue--A Partisan Proposal Based on Strain-range Partitioning", ASTM STP-520, 1973, p. 744-755). Similar trends are suggested in the higher strain rate regime for the R-24 alloy at 0.9% and in the lower strain rate regime for the R-2 alloy at 2.6%.

The N_5 to N_f relation for the data in Tables 3 and 4 appears to be very similar to that observed in Figure 8b. Almost the same conclusion can be stated for the relation between N_i and N_f since the cusp formation in the hysteresis loops was noted in the region close to half-life for all the tests except those in which the strain rates were greater than $2 \times 10^{-3} \text{ sec}^{-1}$. In these higher strain rate tests the cusp formation appeared much later than half-life. This observation must be viewed as only tentative, however, until this phenomenon can be studied in more detail. It is felt, for example, that the response characteristics of the x-y recorder might not be fast enough in these higher strain rate tests to allow the earliest detection of the cusp.

3) Temperature Effects at a Strain Rate of $2 \times 10^{-3} \text{ sec}^{-1}$

A summary of the test results obtained at 482°C and 593°C is presented in Table 5. These data points are shown in Figure 13 and are compared to the curve for 538°C from Figure 8b. It is noted that in the higher strain range regime, little to no temperature effect is apparent but as the strain range is decreased to 0.90 percent a very definite temperature effect begins to appear. A factor of about 2 to 1 in fatigue life is observed at this lower strain range as the temperature is decreased from 593°C to 482°C.

4) Hold-Time Effects at 538°C

The effect of a 300-second hold period on the fatigue life of the R-24 alloy was evaluated at 538°C for two different strain ranges. A summary of the test results obtained is presented in Tables 6 and 7 and is seen to include information relating to a hold period in tension only and a hold period in compression only. A logarithmic plot of fatigue life as a function of total strain range for these hold-time tests is presented in Figure 14 to allow a comparison to be made with continuous cycling results. It is clear that hold periods in tension have a very detrimental effect on fatigue life at this temperature and that the effect seems to increase as the strain range is decreased. Hold periods in compression, on the other hand, do not appear to have any detrimental effect on the fatigue life. As a matter of fact, hold periods in compression in these tests led to fatigue life values which were just slightly greater than those observed in the continuously cycling evaluations. Again, this behavior is completely consistent with the pattern to be expected based on the concept of strainrange partitioning.

An evaluation of the N_5 to N_f relation in Table 6 indicates about the same ratio as obtained for the continuous cycling

Table 5- Low-Cycle Fatigue Test Results Obtained in Argon at 482° and 593° Using a Strain Rate of $2 \times 10^{-3} \text{ sec}^{-1}$

R-24 Series

Marloy 2 (cent. cast, hot-rolled,
solution annealed and aged)

Axial Strain Control

A - ratio of infinity

Spec. No.	Poisson's Ratio	Total Strain Range, %	Freq. cpm	Stress Range at Start, MN/m^2	at $N_f/2$			N_f , Cycles to Failure	N_5 , cycles (see text)
					$\Delta \epsilon_p$, %	$\Delta \epsilon_e$, %	$\Delta \sigma$, MN/m^2		
R-24-33	0.335	0.90	6.67	221	0.69	0.21	200	1253	1150
R-24-34	0.335	2.6	2.3	241	2.36	0.24	228	191	165
R-24-31	0.347	0.90	6.67	321	0.63	0.27	283	2950	2,750
R-24-32	0.335	2.6	2.3	357	2.28	0.32	334	243	195

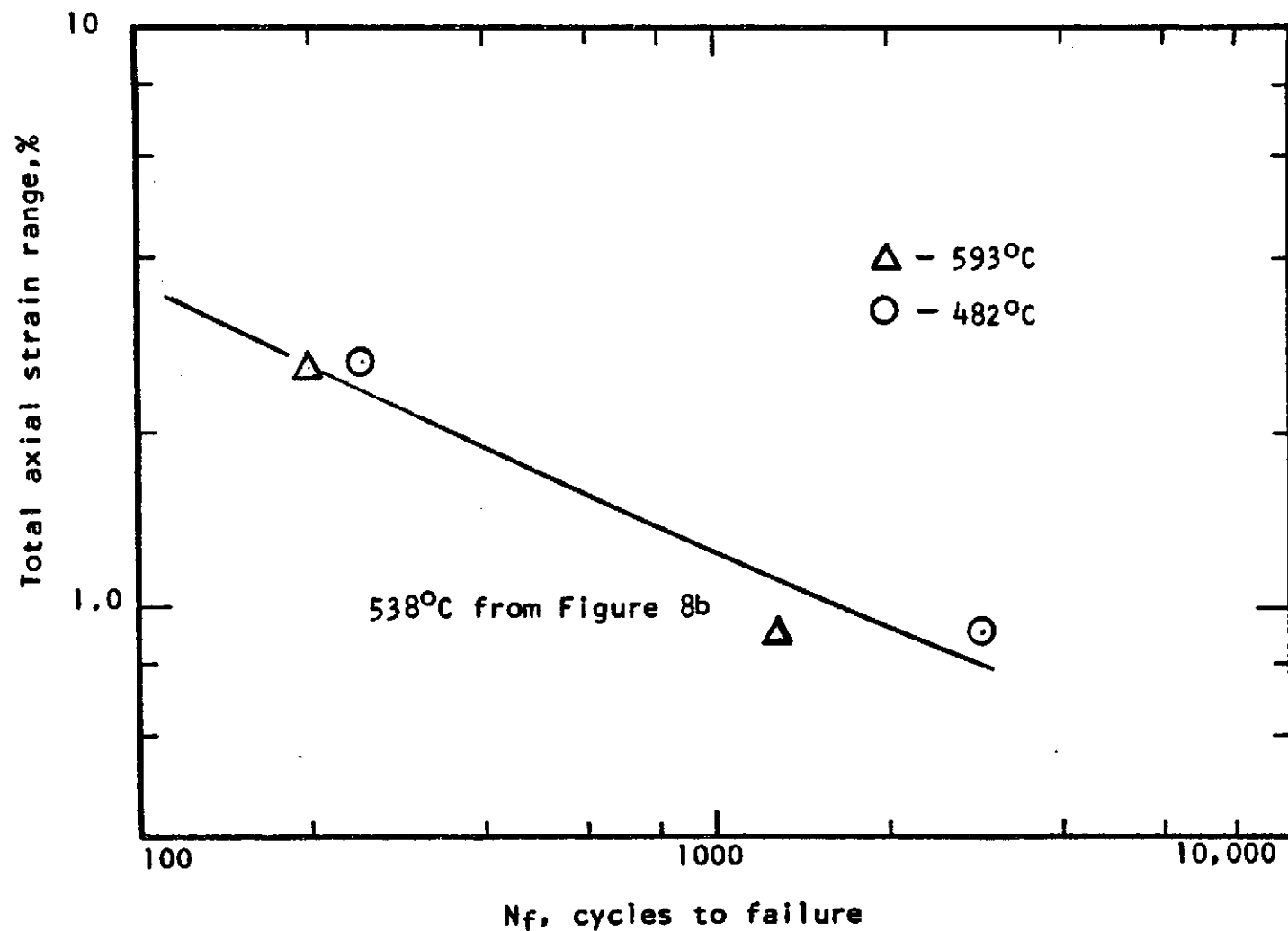


Figure 13 - Effect of temperature on the fatigue life of R-24 alloy tested in argon at a strain rate of $2 \times 10^{-3} \text{ sec}^{-1}$.

Table 6 - Low-Cycle Fatigue Results Obtained in Hold-Time Tests in Argon at 538°C
Using a Ramp Strain Rate of $2 \times 10^{-3} \text{sec}^{-1}$



R-24 Series Marloy Z (cent. cast, hot-rolled, solution annealed and aged)					Axial Strain Control A - ratio of infinity E = $98.6 \times 10^3 \text{ MN/m}^2$		
Spec. No.	Poisson's Ratio	Total Strain Range, %	Cycling Data		N_f , cycles to failure	N_5 , cycles (see text)	Remarks
			Ramp Time, sec.	Hold Time, sec.			
R-24-39	0.33	2.6	26	300, Tension	102	80	 slight initial hardening followed by softening 
R-24-40	0.34	2.6	26	300, Tension	75	55	
R-24-41	0.34	2.6	26	300, Compression	353	290	
R-24-42	0.335	2.6	26	300, Compression	337	280	
R-24-38	0.33	0.90	9	300, Tension	262	205	
R-24-37	0.34	0.90	9	300, Tension	317	252	
R-24-43	0.335	0.90	9	300, Compression	2,981	2350	
R-24-45	0.335	0.90	9	300, Compression	3,392	2750	

Table 7 - Low-Cycle Fatigue Results Obtained in Hold-Time Tests in Argon at 538°C
Using a Ramp Strain Rate of $2 \times 10^{-3} \text{ sec}^{-1}$

R-24 Series

Harley Z (cent. cast, hot-rolled, solution
annealed and aged)

axial Strain Control
A = ratio of infinity
E = $98.6 \times 10^3 \text{ MN/m}^2$

Spec. No.	Stress Range at Start, MN/m^2	at $N_f/2$						
		$\Delta\sigma$ MN/m^2	σ_t MN/m^2	σ_c MN/m^2	σ_r^* MN/m^2	R_σ , Amount of Stress Relaxa- tion, MN/m^2	$\Delta\epsilon_p^{**}$ %	$\Delta\epsilon_e^{**}$ %
R-24-39	303	267	124	143	45T	79T	2.41	0.19
R-24-40	307	271	128	143	52T	76T	2.40	0.20
R-24-41	307	265	127	138	54C	84C	2.42	0.18
R-24-42	302	265	128	137	52C	85C	2.42	0.18
R-24-38	279	232	110	122	50T	60T	0.73	0.17
R-24-37	269	227	110	117	46T	64T	0.73	0.17
R-24-43	272	210	105	105	33C	72C	0.76	0.14
R-24-45	272	214	103	111	36C	75C	0.76	0.14

* T for tension and C for compression; ** Based on relaxed stress range

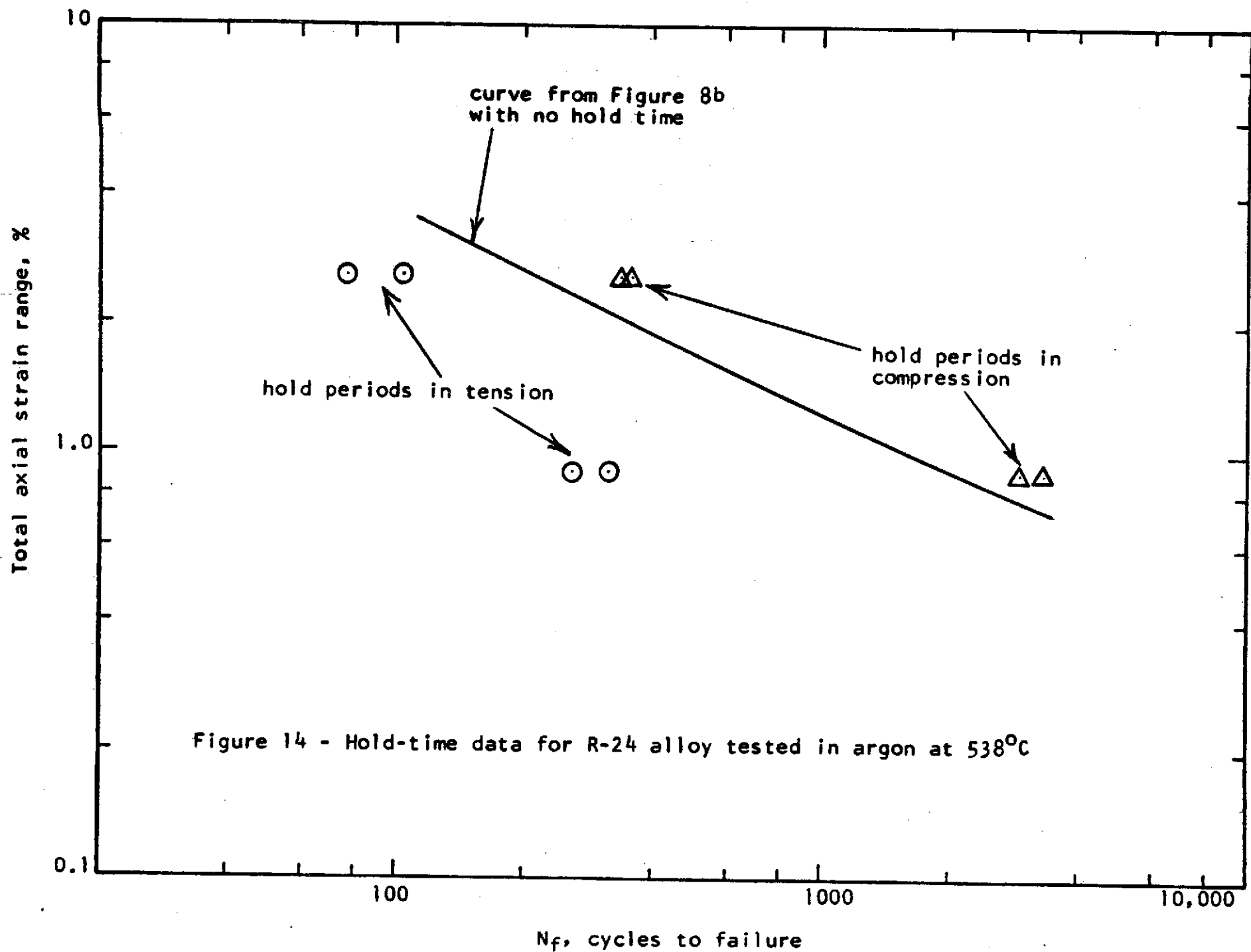


Figure 14 - Hold-time data for R-24 alloy tested in argon at 538°C

tests. It was noted again, however, that the cusp formation occurred before the N_5 point. It was also observed in these hold-time tests that a crack could be identified visibly even before cusp formation was observed.

5) Relaxation Behavior

For each hold-time test the continuous load-time record provided a relaxation curve for each hold period. A typical cycle near half-life was selected from each hold-time tests and load-time combinations were chosen at various intervals throughout the hold period to define the relaxation curves presented in Figures 15 through 20. These curves along with the R_σ data in Table 7 enable some comparison to be made of the relaxation behavior exhibited in the several different tests performed in this program. Actually no large differences in relaxation characteristics are in evidence and the difference between tension and compression relaxation appears slight.

It can be noted that the relaxation behavior exhibited in duplicate tests defines essentially identical results (the relaxation curves at half-life for R-24-41 and R-24-42 were identical and are shown as such in Figure 16). It can also be noted that the R_σ values for the R-24-41 and R-24-42 tests are slightly higher than those observed in the R-24-39 and R-24-40 tests but this appears reasonable in view of the higher initial stress levels in the -41 and -42 tests. A similar data trend is also observed in the R_σ values for the tests at a strain range of 0.90% even though the initial stress levels are about the same in both the tension-hold and compression-hold tests. There is no explanation for this behavior pattern at this time but the relatively long duration of the compression-hold tests at the 0.90% strain range might have some bearing on this phenomenon. When all the relaxation curves in the Table 6 tests were compared at the tenth cycle of the test it was noted that the behavior patterns at the same strain range were very similar for the compression and tension hold periods.

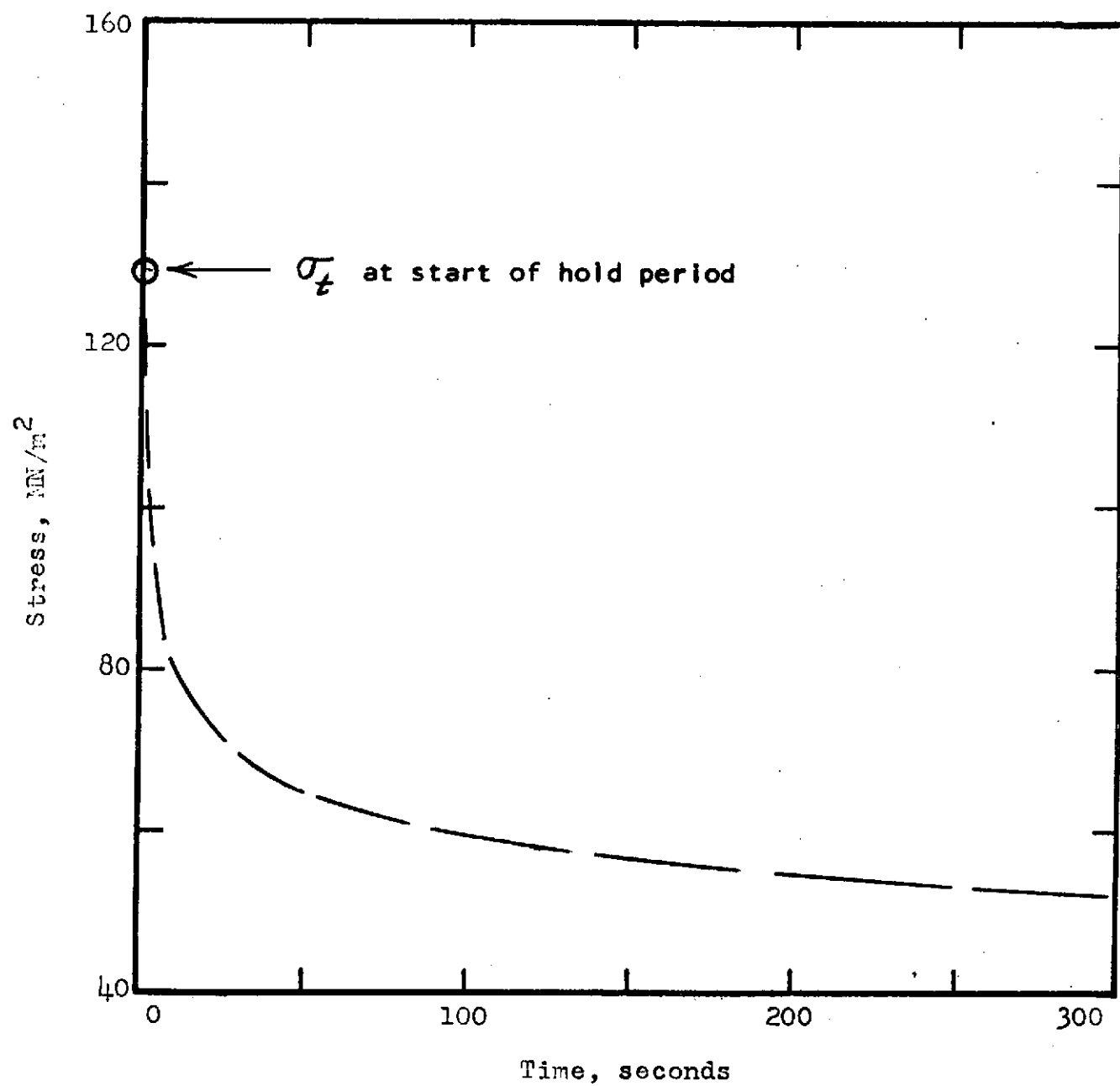


Figure 15 - Relaxation curve near $N_f/2$ for spec. No. R-24-40

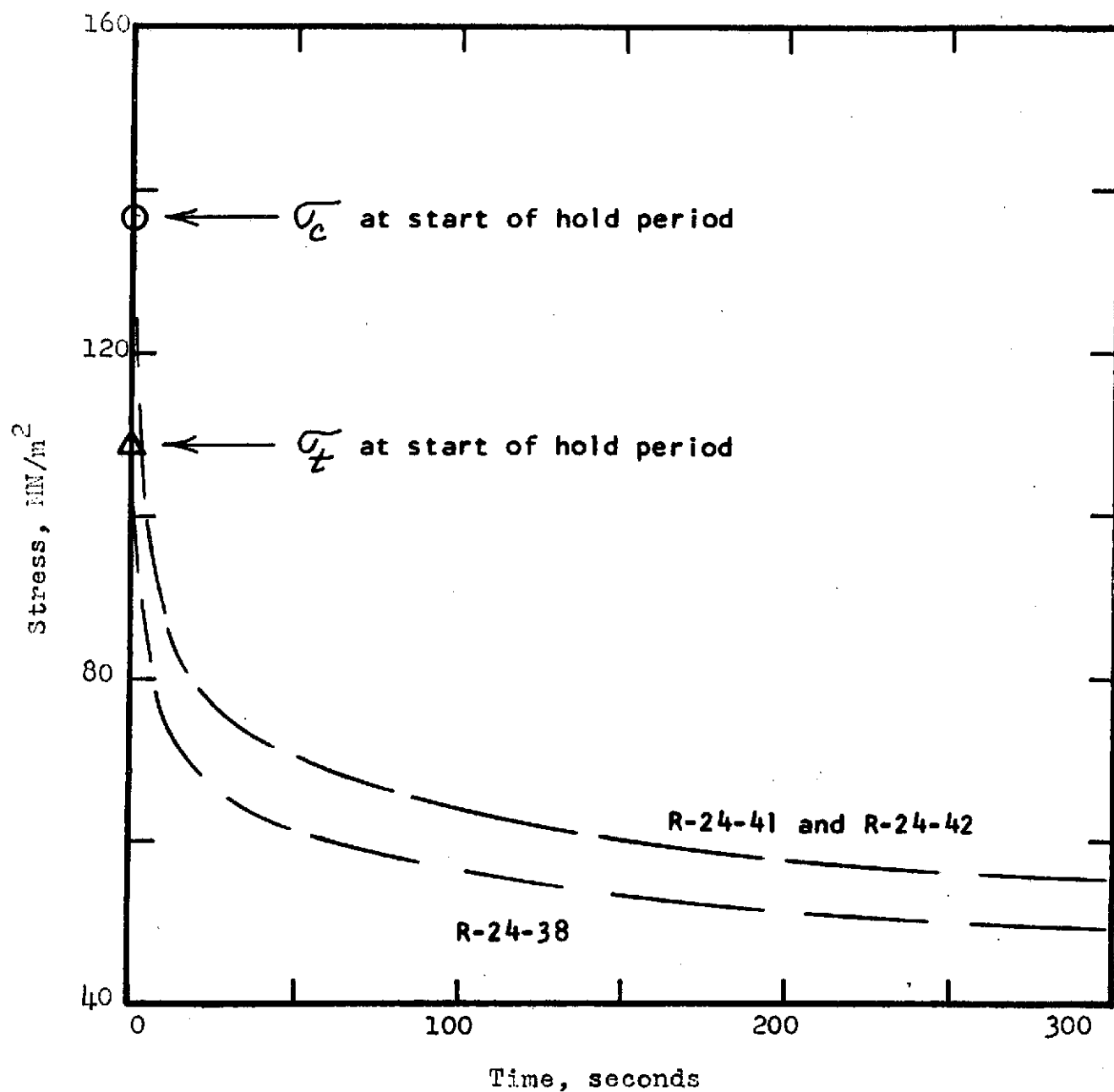


Figure 16- Relaxation curves near $N_f/2$ for Spec. Nos. R-24-41, R-24-42 and R-24-38

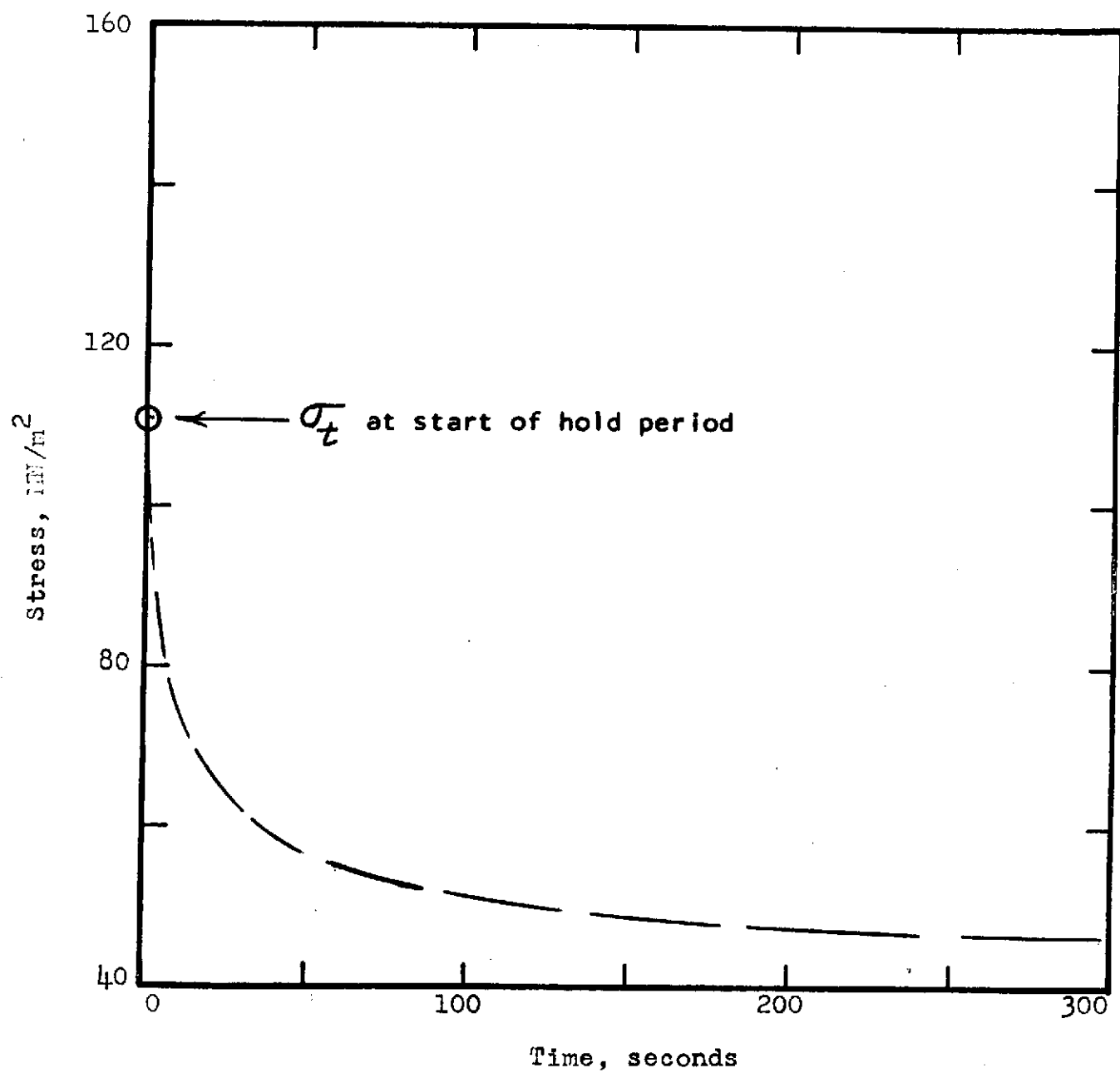


Figure 17- Relaxation curve near $N_f/2$ for Spec. No. R-24-37

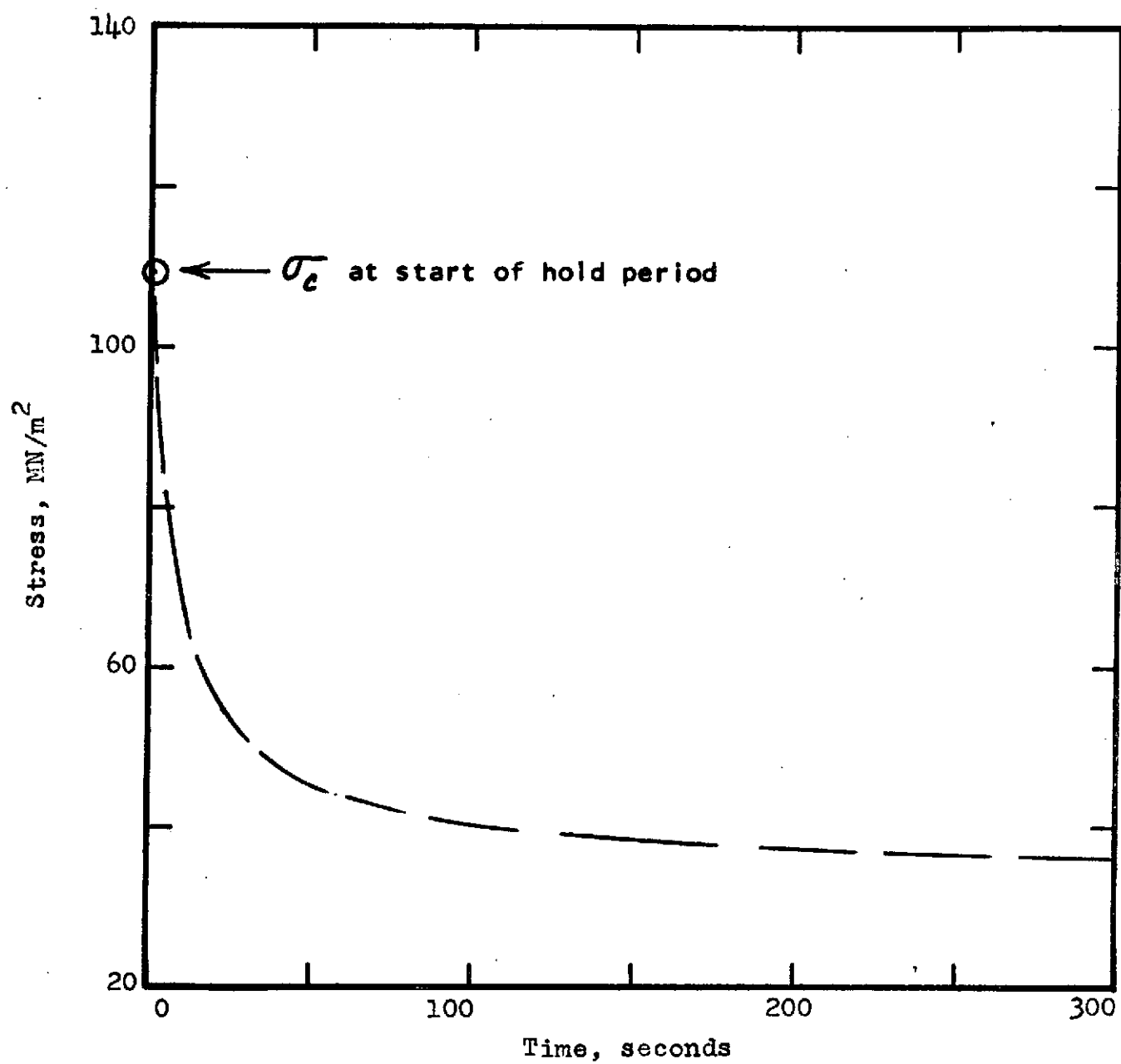


Figure 18- Relaxation curve near $N_f/2$ for spec. No. R-24-45

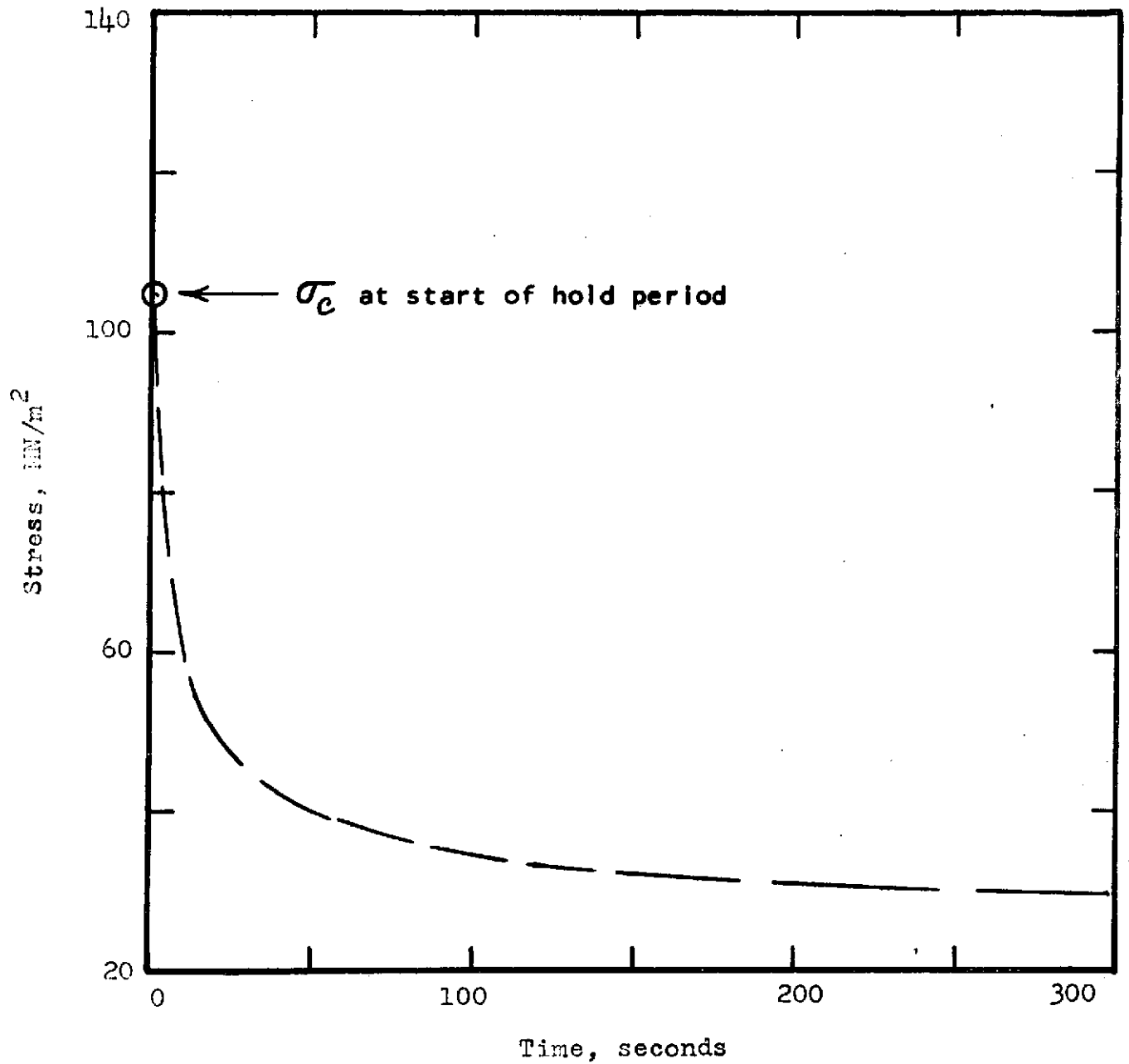


Figure 19- Relaxation curve near $N_f/2$ for Spec. No. R-24-43

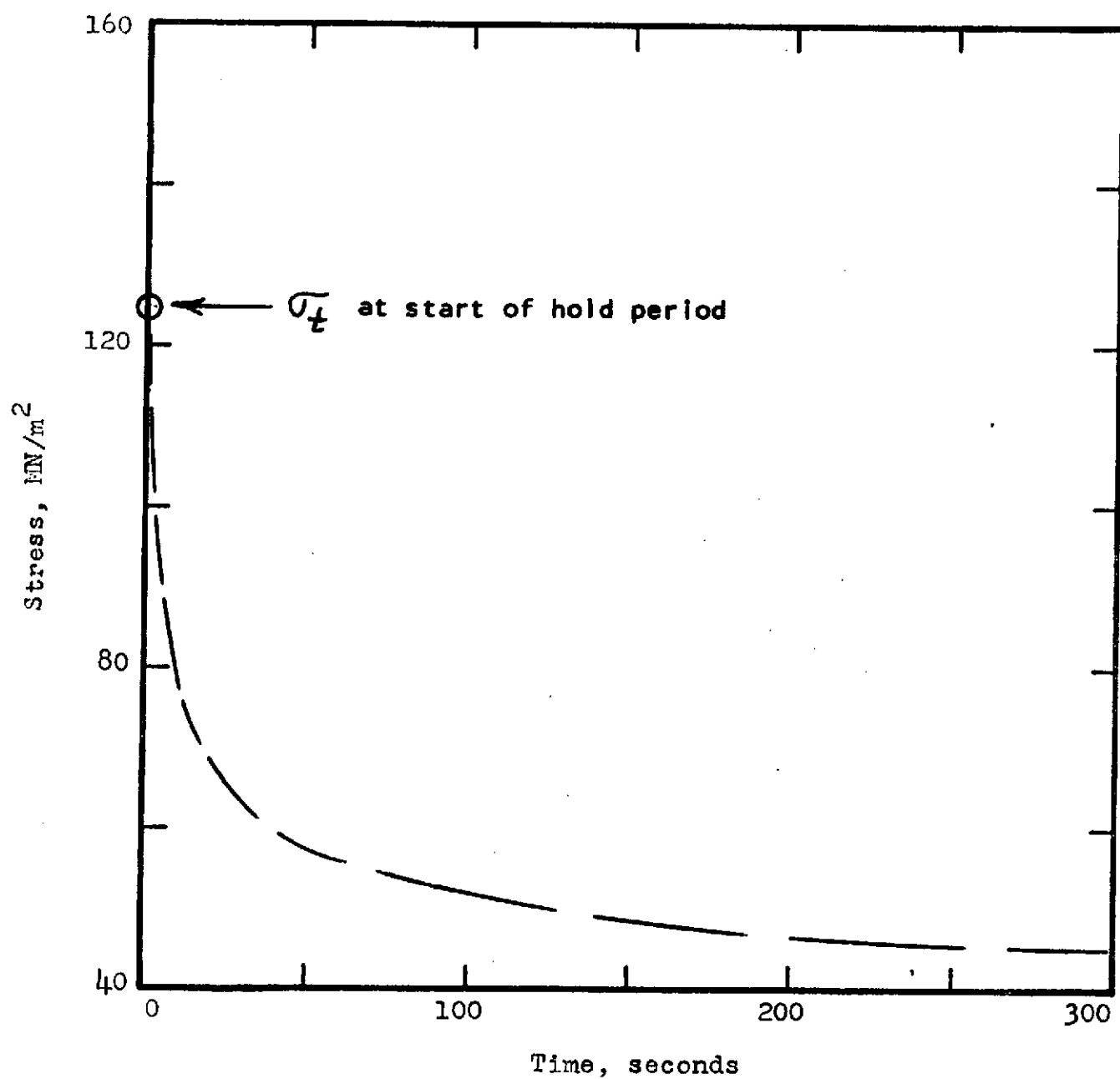


Figure 20- Relaxation curve near $N_f/2$ for Spec. No. R-24-39

VII- CONCLUSIONS

This report presents a detailed summary of the test results obtained in an evaluation of the short-term tensile and low-cycle fatigue behavior of the copper-base alloy, Narloy Z (an alloy developed by North American Rockwell for possible application as a reusable rocket nozzle liner material). This material was tested in the centrifugally cast, hot-rolled, solution annealed and aged condition with all the room temperature evaluations performed in air and the elevated temperature tests performed in high purity argon.

Short-term tensile tests performed at room temperature, 482° and 538° and 593°C using an axial strain rate of $2 \times 10^{-3} \text{ sec}^{-1}$ revealed ultimate and yield strength values at room temperature of 315 and 200 MN/m² respectively which gradually decreased to 120 and 105 MN/m² respectively as the temperature increased to 593°C. Over this same temperature regime the reduction in area values ranged from about 50 percent at room temperature and 482°C to a value of about 41 percent at 538°C and to a value of about 46 percent at 593°C. Strain rates ranging from 4×10^{-4} to $1 \times 10^{-2} \text{ sec}^{-1}$ seemed to have very little effect on ultimate and yield strength at a test temperature of 538°C but led to an increase in reduction in area values from about 35 to 50 percent as the strain rate was increased.

Axial strain-controlled low-cycle fatigue tests of the R-24 alloy were performed in argon at 538°C and a strain rate of $2 \times 10^{-3} \text{ sec}^{-1}$ to define the cyclic life over the range from 100 to 3000 cycles. In addition to reporting the number of cycles to failure for each test a value of N_5 , the number of cycles to a 5 percent reduction in tensile load below the steady state value, was identified. The ratio of N_5 to N_f was close to 0.82 over the entire strain range studied.

Other fatigue tests of the R-24 alloy were performed at 538°C to evaluate strain rate effects at strain ranges of 0.90 and 2.6 percent. It was found that the fatigue life showed a definite tendency toward saturation at both the low ($4 \times 10^{-4} \text{ sec}^{-1}$) and the high ($5.2 \times 10^{-2} \text{ sec}^{-1}$) strain rate.

The effect of temperature on the fatigue life of the R-24 alloy was evaluated at strain ranges of 0.90 and 2.6 percent over the temperature range from 482° to 593°C. Little to no temperature effect was observed at the higher strain range but the fatigue life increased by a factor of about 2.0 at a strain range of 0.90 percent as the temperature decreased from 593° to 482°C.

Hold period durations of 300 seconds were employed at 538°C in tests at strain ranges of 0.90 and 2.6 percent. Hold periods in only the tension portion of the cycle were found to be very detrimental and led to substantial reductions in the fatigue. Hold periods in compression only were not found to be detrimental at all and yielded fatigue life values that were slightly greater than those observed in continuously cycling tests at the same temperature and strain range.

Relaxation behavior observed during the hold periods was found to be essentially the same in tension and compression.

THE FOLLOWING PAGES ARE DUPLICATES OF
ILLUSTRATIONS APPEARING ELSEWHERE IN THIS
REPORT. THEY HAVE BEEN REPRODUCED HERE BY
A DIFFERENT METHOD TO PROVIDE BETTER DETAIL